Progress in Oceanography 219 (2023) 103133

Contents lists available at ScienceDirect

Progress in Oceanography

journal homepage: www.elsevier.com/locate/pocean

Atlantification influences zooplankton communities seasonally in the northern Barents Sea and Arctic Ocean

Anette Wold [a,*], Haakon Hop [a], Camilla Svensen [b], Janne E. Søreide [c], Karen M. Assmann [d], Mateusz Ormanczyk [e], Slawomir Kwasniewski [e]

[a] Norwegian Polar Institute, 9296 Tromsø, Norway
[b] Department of Arctic and Marine Biology, UiT the Arctic University of Norway, 9037 Tromsø, Norway
[c] University Centre in Svalbard, 9171 Longyearbyen, Norway
[d] Institute of Marine Research, 9296 Tromsø, Norway
[e] Institute of Oceanology, Polish Academy of Sciences, 81-712 Sopot, Poland

ARTICLE INFO

Keywords:
Zooplankton diversity
Arctic copepods
Warming Arctic
Seasonality
Ecosystem
Climate change

ABSTRACT

The Barents Sea is undergoing rapid ocean warming with less sea ice and increased Atlantic inflow, shifting the pelagic ecosystem towards a more boreal one, a process referred to as Atlantification. While such changes have already been documented in the southern and central Barents Sea, less is known about the degree of Atlantification in the northern Barents Sea and Arctic Ocean. In this seasonal study, we identified the mesozooplankton biodiversity, abundance and biomass in the Northern Barents Sea along a transect with seven stations stretching from the central Barents Sea (76°N) across the shelf break and into the Arctic Ocean (82°N) in August and December 2019, and March, May and July 2021. The broad range of mesozooplankton taxa and sizes were collected by conducting duplicate depth-stratified tows using alternate nets of mesh-sizes 64 μm and 180 μm. The majority of zooplankton taxa were ubiquitous in the study area, but the abundances and life stages varied depending on the season, region and the dominant water mass. We identified three distinct biogeographical regions with different zooplankton diversity and seasonal dynamics; (i) south of the Polar Front, (ii) northern Barents Sea shelf, and (iii) shelf slope and Arctic Ocean. During summer, high abundances of Atlantic/boreal and cosmopolitan zooplankton, mainly *Calanus finmarchicus*, *Metridia longa*, *Oithona similis* and *Microsetella norvegica* were found just south of the Polar Front in the central Barents Sea. On the shelf, Arctic species, such as *Calanus glacialis*, *Pseudocalanus* spp., and *Limacina helicina* dominated year-round with relatively high and stable biomass. At the northernmost stations, peaks of *C. finmarchicus* and Oncaeidae (*Triconia borealis* and *Oncaea* spp.) occurred in winter, combined with bathypelagic species such as *Paraeuchaeta* spp., *Scaphocalanus brevicornis, Spinocalanus* spp., *Gaetanus brevispinus* and *Heterorhabdus norvegicus*. Hence, when comparing the mesozooplankton communities at the different locations and seasons, four distinct communities were identified: shelf winter, shelf spring, shelf summer, and Arctic Ocean. Stronger advection and increased northward expansion of Atlantic zooplankton species are anticipated in the future, which could impact the diversity of the more endemic and energy-richer Arctic zooplankton communities.

1. Introduction

The Arctic experiences distinct climate-change effects including the reduction of the extent and thinning of existing summer sea ice due to warming (Stroeve and Notz, 2018) and changes in timing and duration of the productive season (Dalpadado et al., 2014; Renaut et al., 2018; Rantanen et al., 2022). These changes may alter marine ecosystems by inducing structural and functional changes from phytoplankton to zooplankton to higher trophic levels (Arrigo and van Dijken, 2015; Pedersen, 2022). The northern Barents Sea is an area where the impact on the ecosystem may be particularly severe, as the total sea-ice cover area has decreased compared to the 1981–2020 mean extent (Lind et al., 2018; Stroeve and Notz, 2018). Also, the northern Barents Sea shelf and the Eastern Fram Strait are the two main inflow systems through which warm and nutrient-rich Atlantic Water (AW) is transported into the Arctic Ocean (Beszczynska-Möller et al., 2012; Ingvaldsen et al., 2021;

* Corresponding author.
E-mail address: anette.wold@npolar.no (A. Wold).

https://doi.org/10.1016/j.pocean.2023.103133

Available online 29 September 2023

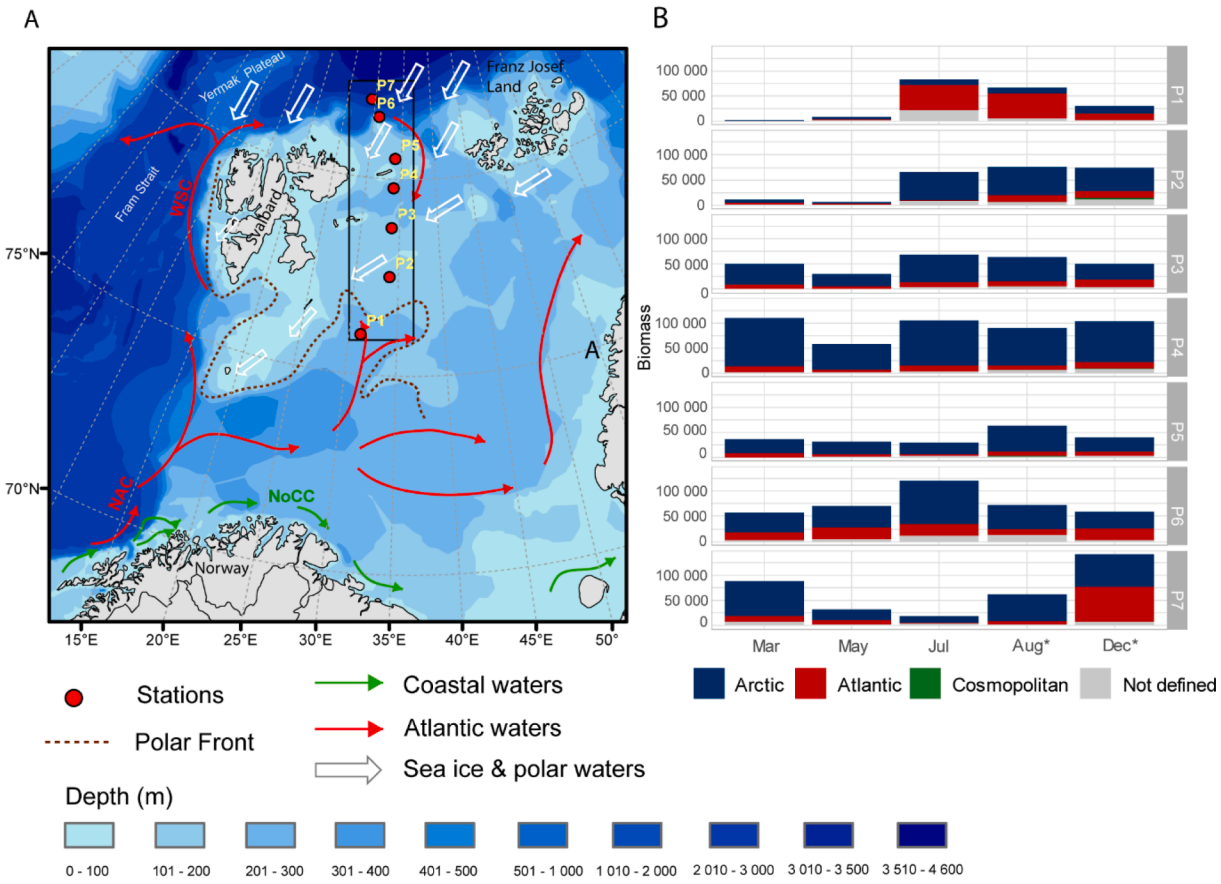

Fig. 1. (A) Sampling stations (red circles) visited during the seasonal surveys in 2019 and 2021 in the northern Barents Sea. The current system including NAC (Norwegian Atlantic Current), NoCC (North Cape Current), and WSC (West Spitsbergen Current) is depicted by arrows in colours of their respective water masses. (B) The total mesozooplankton biomass (mg DM m^{-2}) in March, May, July, August and December (* = 2019, all other months in 2021) was grouped into representing Arctic, Atlantic, Cosmopolitan and not defined (due to the impossibility of determining biogeographical affiliation because of low taxonomical resolution or identification) taxa. The figure is modified from Fig. 1 in Van Engeland et al. (2023).

Polyakov et al., 2023). The arrival of this relatively warm water impacts the regional ecosystem (Wassmann et al., 2019), especially the pelagic realm, as the presence of Atlantic species alters the plankton community composition (Wassmann et al., 2006, 2015), including zooplankton, with consequences for other biotas (Falk-Petersen et al., 2007; MacKenzie et al., 2022). This process is referred to as Atlantification, with underlying mechanisms being ocean advection and air-sea heat fluxes acting in concert to drive the periodical warming in the upper ocean (Asbjørnsen et al., 2020; Polyakov et al., 2023).

In the European Arctic, the increased contributions of Atlantic zooplankton are linked to positive temperature anomalies caused by an increase in transport and temperature of the Atlantic Water (Dalpadado et al., 2012; Gluchowska et al., 2017; Mańko et al., 2020; Polyakov et al., 2023). The inflowing Atlantic Water carries biota and particles, but also heat as a driver of environmental change, which tends to favour advected Atlantic species (Ingvaldsen et al., 2021). Sympagic organisms are also being eliminated from their habitats in surface waters because of the melting and shrinking of sea ice, which results in the impoverishment of the surface zooplankton communities (Kunisch et al., 2020; Ershova et al., 2021; Hop et al., 2021a).

At high latitudes, the seasonality of zooplankton communities is mainly driven by the pulsed primary production that takes place when light and nutrients become available in stratified surface layers in the wake of sea-ice melt (Leu et al., 2015). Seasonal changes in sea ice conditions will impact the underwater light and nutrient regimes due to altered exposure of the water column to atmospheric forcing (Ingvaldsen et al., 2021). These altered light and nutrient regimes may cause changes in the onset, length and intensity of the ice algae and phytoplankton blooms, which again impact the grazers (Søreide et al., 2010; Leu et al., 2011; Dalpadado et al., 2020; Duarte et al., 2021). The altered light and nutrient conditions may also affect the community composition of primary producers (Leu et al., 2010; Ji et al., 2012; Ardyna and Arrigo, 2020), with implications for the nutritional quality of the phytoplankton, and ultimately the first-order consumers.

Copepods comprise the majority of the mesozooplankton in the Arctic. On a global scale, copepod spatial diversity peaks in sub-tropical regions and declines towards the poles (Rombouts et al., 2009). Further, Rombouts et al. (2009) showed that local species diversity appears to be dependent on temperature and chlorophyll *a* concentration (i.e., phytoplankton biomass) which are both sensitive to climate change. Since temperature and phytoplankton biomass are important drivers in the Arctic, zooplankton abundance and biomass increase during the primary production period, particularly for the lipid-rich copepods *Calanus* spp., which reach critical size and enter diapause at the end of summer. Their descent may shift the zooplankton communities' diversity and create a niche for smaller and less lipid-rich organisms with different overwintering strategies (Lischka and Hagen, 2005, 2007; Balazy et al. 2021). This change in zooplankton biodiversity from early spring to late summer has been observed (Walkusz et al., 2009; Weydmann et al., 2013), but few studies have investigated seasonal patterns of zooplankton diversity during all seasons, with a focus on all copepod size groups from tiny nauplii to large adult of *Calanus hyperboreus*.

In this study, we investigate the mesozooplankton communities in the northern Barents Sea, from south of the Polar Front in the Central Barents Sea, across the northern Barents Sea shelf into the deep Arctic Ocean (76–82 N), during summer, autumn, winter and spring. We aim to

identify the seasonality of Arctic and Atlantic zooplankton communities to evaluate the impact of Atlantification. The description of mesozooplankton community was obtained by combining 64 μm and 180 μm mesh depth-stratified net samples to capture a broad range of size groups from small copepod nauplii and meroplanktonic larvae to large copepod species and pelagic amphipods and chaetognaths. We hypothesise that the diversity, abundance and biomass of zooplankton 1) change with seasons and 2) is higher in areas impacted by Atlantic Water than in areas dominated by more local Arctic water masses.

2. Material and method

2.1. Study area

Material for this study was collected during five surveys with R/V *Kronprins Haakon* covering all four seasons. The summer and late autumn surveys (Q3 and Q4) were performed on 5–27 August and 28 November – 17 December 2019, whereas those from late winter, spring and summer (Q1,Q2 and JC2-1) were postponed until 2–25 March, 27 April – 20 May 2021 and 12 July – 29 July 2021, respectively. However, postponing cruises one year also introduced interannual difference as a factor for the difference observed between seasons. Sampling and measurements were carried out along the transect from the central Barents Sea (76° N) to the Arctic Ocean (82° N), at seven stations (P1 to P7; Fig. 1). The Barents Sea is strongly influenced by warm Atlantic Water (AW), which splits into two distinct branches at the southwestern boundary of the Barents Sea (Fig. 1 A). A wide inflow enters the southern Barents Sea through Bear Island Trough and dominates water mass characteristics on the Barents Sea south of the Polar Front. In the western Barents Sea, our region of interest, the position of the Polar Front is largely constrained by bathymetry (Våge et al., 2014; Oziel et al., 2016) and it was crossed by our section at the Hopen Saddle between stations P1 and P2. A narrow core of AW follows the shelf break northwards as part of the West Spitsbergen Current. Part of this core enters the Arctic Basin through Fram Strait and across the Yermak Plateau to continue along the shelf break north of Svalbard as the Atlantic Water Boundary Current (Crews et al., 2019). AW from this current enters the Barents Sea shelf from the north through the Kvitøya and Franz Victoria Troughs (Lind and Ingvaldsen, 2012; Lundesgaard et al., 2022).

Therefore, the meridional section presented in this study included stations with varying degrees of Atlantic influence. The southernmost station (P1) was permanently located south of the Polar Front and therefore experienced strong AW influence during all cruises. Stations P2 to P5 were located north of the Polar Front on the continental shelf in an area with a pronounced presence of polar water masses while the station at the shelf break (P6) was in the Atlantic Water Boundary Current (Renner et al., 2018). The northernmost station (P7) was situated in the deep Nansen Basin with Polar Water in the surface layer, modified AW at intermediate depth and cold and salty Atlantic Intermediate Water below 600 m.

2.2. Zooplankton sampling

Zooplankton were sampled with stratified vertical net hauls using two separate MultiNet Midi (HydroBios, opening: 0.25 m^2, net length: 2.50 m), one with 64 μm and one with 180 μm mesh nets to cover all size groups of mesozooplankton, at five standard depth intervals. The depth intervals at the shallow shelf stations (P1-P5) were from close to the bottom-200 m, 200–100 m, 100–50 m, 50–20 m, and 20–0 m. At the shelf break (P6) and deep station (P7), the sampling depths were from 1000 to 600, 600–200, 200–50, 50–20, and 20–0 m. All samples were processed immediately upon retrieval of the nets. The zooplankton were concentrated on sieves (64 μm and 180 μm respectively), gently flushed with filtered seawater before being transferred into 125 mL plastic bottles and preserved in 4 % formaldehyde free from acid.

2.3. Zooplankton analysis

The zooplankton organisms were identified and counted under a stereomicroscope equipped with an ocular micrometre according to standard procedures (Postel, 2000). Small-sized zooplankters (total size < 5 mm, including most of Copepoda, and juvenile stages of Pteropoda, Euphausiacea, Ostracoda, Amphipoda, and Chaetognatha) were identified and counted in sub-samples taken from a fixed sample volume using automatic macro pipette, and in this procedure, not less than 500 individuals from not less than five sub-samples were always identified and counted. Large zooplankters (total size > 5 mm, including big Copepoda, Pteropoda, Euphausiacea, Ostracoda, Amphipoda, Decapoda, Appendicularia, Chaetognatha, and Pisces larvae) were sorted and identified from the whole sample. Representatives of *Calanus* spp. were identified at the species level based on morphology and prosome lengths of individual copepodid stages (Kwasniewski et al., 2003). The samples from the 64 μm and 180 μm gauze nets were analysed separately, and the analytical results were then combined, taking occurrence and abundance data for small taxa and stages from the 64 μm net and data on larger taxa and stages from the 180 μm net samples. A list of species and stages with information from which net data were used for analyses is provided in Supplementary Table 1.

2.4. CTD and other environmental variables

A shipboard conductivity, temperature, and depth profiler (Seabird 911plus CTD), attached to a 24-bottle rosette system was deployed at all sampling stations. For inclusion in the multivariate analyses, average values of potential temperature (T), practical salinity (S) and potential density anomaly (σ_θ) were calculated for each of the layers of the zooplankton samplings. We used the definitions by Sundfjord et al. (2020) for water mass classification. Sea-water samples for chlorophyll *a* concentration were taken from water bottles mounted on the rosette system, collecting water during the CTD deployments. Samples of 100–500 mL were filtered through 25 mm GF/F filters (Whatman), extracted in 100 % methanol for 12 h at 4 °C and measured with a Trilogy Laboratory Fluorometer (Turner Design, San Jose, CA, USA) according to the method of Holm-Hansen and Riemann (1978).

Sea-ice concentration (SIC) during the surveys was calculated based on daily sea-ice concentrations from Nimbus-7 SMMR and DMSP SSM/I-SSMIS Passive Microwave Data received from NSIDC (Cavalieri et al., 1996).

2.5. Zooplankton community structure

Original zooplankton data present the abundance of zooplankters (ind. m^{-3}) in each sampled depth layer. Abundance values were converted to biomass estimates (mg dry mass m^{-3}, mg DM m^{-3}) using species-specific dry mass values gathered from published sources or measured by the authors (Supplementary Table 1). The abundance and biomass of each organism at a station, ind. m^{-2}, mg DM m^{-2}, respectively, were calculated by summing the abundance or biomass in each layer for the whole water column (Figs. 5-12).

The zooplankton community structure and diversity were explored by examining zooplankton similarity using hierarchical cluster analysis on 4^{th} root transformed abundance data including life stages and size groups (ind. m^{-2}), which dampens the effects of dominant taxa in the Bray–Curtis similarity, using PRIMER (version 7.021). ANOSIM analysis was used to test for differences in zooplankton community composition between distinct clusters (PRIMER, version 7.021; Clarke and Gorley, 2015).

The relation between the overall zooplankton composition at stations and different environmental variables was explored using a Canonical Correspondence Analysis (CCA, CANOCO version 5) of 4^{th} root transformed abundance data including life stages and size groups (ind. m^{-2}). This is a constrained ordination, which maximises the

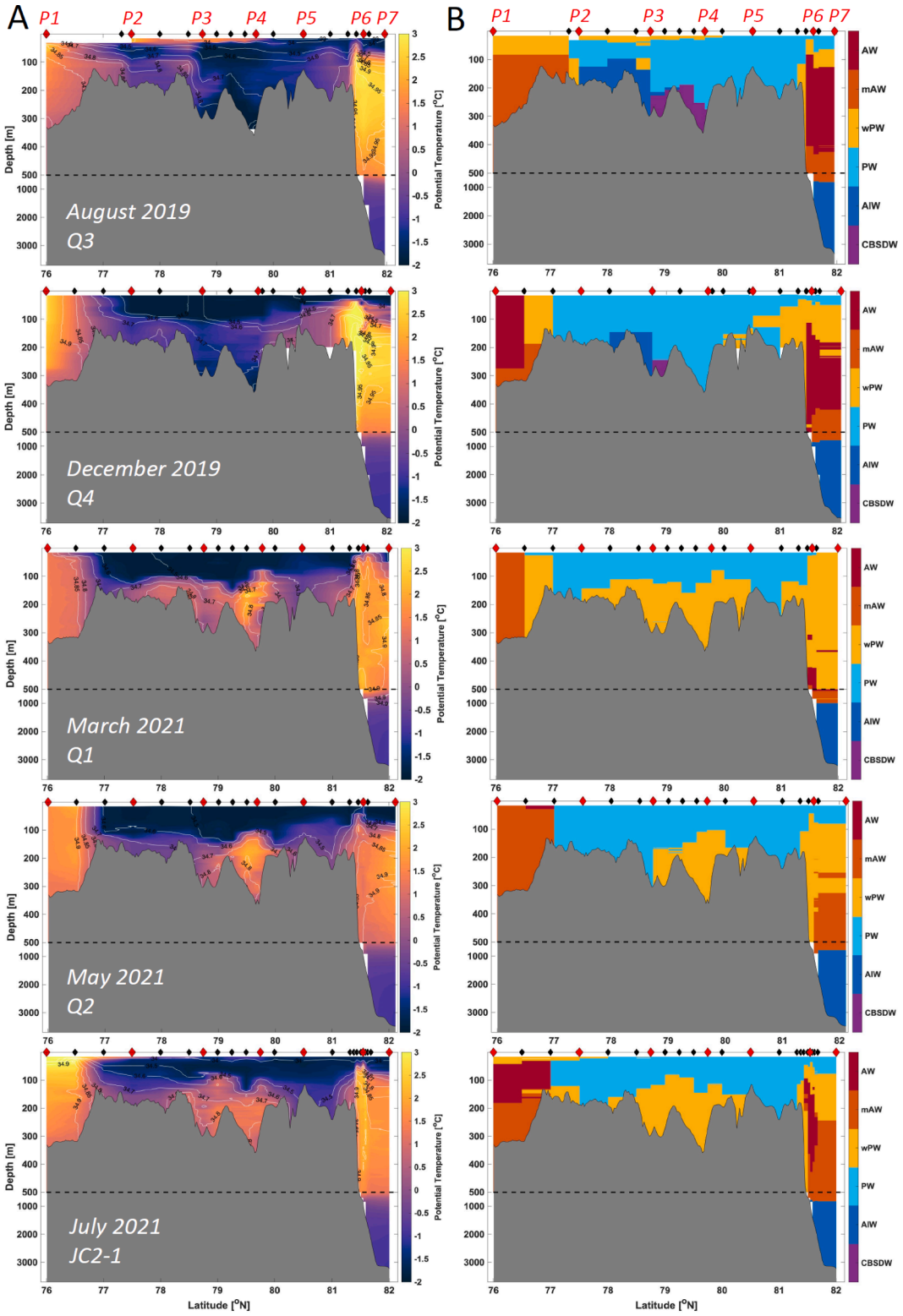

Fig. 2. Hydrographic sections for all seasonal cruises. (A) Potential temperature (colour-coded) and practical salinity (contours). (B) Water mass classifications according to Sundfjord et al. (2020). AW = Atlantic Water, mAW = modified Atlantic Water, PW = Polar Water, wPW = warm Polar Water, AIW = Arctic Intermediate Water, CBSDW = Central Barents Sea Dense Water. Red diamonds mark stations P1 to P7, smaller black diamonds intermediate hydrographic stations without zooplankton sampling. Note that the vertical depth axis is compressed below 500 m.

relationships between taxa and environmental variables. In total 192 taxa and size groups were included in the analysis, but only the 50 best-fitted taxa are shown in the figure in order to maintain the readability of the results. The following environmental variables were included; latitude, bottom depth (m), mean chlorophyll *a* standing stock in the upper 50 m (log transformed), the mean temperature in the upper 50 m (log transformed), mean salinity in the upper 50 m, relative sea-ice coverage and day of the year. The environmental variables were

Table 1
Overview of stations and physical parameters. The predominant water masses, indicated for each station, are Atlantic Water (AW), modified Atlantic Water (mAW; T > 0 °C, S > 34.9), Polar Water (PW; T < 0 °C, σ_θ < 27.97 kg m^{-3}), and Warm Polar Water (wPW; T > 0 °C, S < 34.9).

Station	Date	Time (64 µm)	Time (180 µm)	Predominant water mass	Bottom depth (m)	Longitude (°N)	Latitude (°E)	Temperature (°C)	Salinity (psu)	Chl *a* 0–50 m (mg m^{-2})	Ice cover (% coverage)
Seasonal cruise Q3 - August 2019											
P1	08/08	12:17	12:55	mAW/wPW	323	31.2201	76.0000	2.482	34.818	25.263	0
P2	12/08	03:53	03:19	wPW	186	33.9864	77.5006	0.099	34.417	38.807	0
P3	13/08	06:58	06:20	PW	306	34.0000	78.7500	−0.642	34.417	18.157	0
P4	14/08	10:10	08:33	wPW	343	34.2245	79.7073	−0.991	34.327	28.822	19
P5	16/08	04:49	04:12	PW	160	34.0835	80.4884	−1.451	34.234	73.040	67
P6	18/08	20:26	18:33	wPW/mAW	849	31.4993	81.5604	0.322	34.367	330.260	75
P7	20/08	16:05	14:58	wPW/mAW	3300	29.7287	81.9811	0.013	34.470	43.645	73
Seasonal cruise Q4 - December 2019											
P1	12/12	21:18	20:22	AW	326	31.2190	75.9996	2.452	34.950	1.760	94
P2	10/12	20:14	19:25	PW	192	33.9974	77.5003	−1.569	34.529	0.766	92
P3	09/12	22:39	23:25	PW	306	33.9934	78.7502	−1.643	34.593	0.517	92
P4	08/12	17:53	09:51	PW	346	33.9890	79.7220	−1.495	34.354	0.722	92
P5	07/12/2019	01:30	01:03	PW	147	34.2602	80.5149	−0.894	34.317	0.710	77
P6	05/12	04:45	16:05	wPW/mAW	907	30.8118	81.5495	0.682	34.485	1.859	28
P7	02/12	21:21	17:49	wPW	3150	28.5876	82.0486	−0.189	34.192	2.075	1
Seasonal cruise Q1 - March 2021											
P1	05/03	14:25	14:18	wPW/mAW	325	31.2197	76.0000	1.426	34.898	0.455	0
P2	07/03	06:34	07:17	PW	188	33.9705	77.5042	−1.502	34.555	0.422	86
P3	08/03	17:57	18:40	wPW/mAW	303	34.0051	78.7569	−1.020	34.508	0.427	94
P4	10/03	16:27	17:07	PW/wPW	339	33.6231	79.7602	−0.354	34.544	0.433	91
P5	12/03	14:12	14:29	PW	154	34.1277	80.4894	−1.231	34.423	0.441	84
P6	15/03	18:38	15:24	wPW/AW	802	32.0251	81.5620	0.946	34.786	0.652	67
P7	16/03	00:59	21:22	wPW/mAW	3298	29.9964	82.0020	−0.142	34.702	0.756	63
Seasonal cruise Q2 - May 2021											
P1	30/04	13:54	13:18	mAW	326	31.2198	76.0000	1.635	34.914	75.768	0
P2	02/05	09:58	10:31	PW	186	33.9660	77.4992	−1.583	34.581	56.527	32
P3	03/05	22:44	23:27	PW	314	33.9460	78.7343	−1.110	34.556	20.664	71
P4	05/05	00:53	00:21	wPW	339	33.9546	79.7420	−0.492	34.521	88.292	77
P5	07/05	23:32	23:09	PW	173	34.0162	80.5269	−1.278	34.419	24.893	90
P6	10/05	03:41	02:19	wPW/mAW	1611	30.6076	81.5686	0.109	34.734	99.758	87
P7	14/05	11:41	07:39	wPW/mAW	3316	29.7511	82.0253	−0.347	34.645	12.839	92
Joint Cruise 2–1 - July 2021											
P1	14/07	13:03	20:16	wPW/mAW	323	31.2195	76.0000	2.698	34.906	68.856	0
P2	15/07	13:32	19:13	PW	188	34.0005	77.5001	−0.759	34.340	8.534	0
P3	17/07	07:48	08:58	PW	303	34.0008	78.7501	−0.520	34.261	28.709	0
P4	18/07	12:04	13:50	PW	332	34.0000	79.7500	−0.356	34.345	112.226	0
P5	19/07	08:14	08:35	PW	161	33.9606	80.5020	−1.480	34.196	119.145	98
P6	22/07	19:13	20:44	wPW/mAW	986	30.7683	81.5487	0.297	34.499	72.331	93
P7	24/07	13:00	11:20	wPW/mAW	3296	30.0666	81.9861	−0.234	34.438	12.317	100

tested using a forward selection with 499 runs, and the relative contribution (% value) and significance (*p*-value) were used to select the most relevant explanatory variables (Table 3). The results of the CCA is displayed in a biplot showing samples and environmental variables where the distance between the symbols (samples of individual zooplankton communities from a station) approximates the dissimilarity of their taxa composition as measured by the chi-square distance. The environmental variables are shown as arrows pointing in the direction of the steepest increase of environmental variables. The taxa are displayed in a separate scatter plot where the distance between the symbols (taxa) approximates the dissimilarity of distributions of relative abundance of those taxa across the samples as measured by the chi-square distance. Taxa placed in proximity on the plot are taxa that often occur together in the natural space (Šmilauer and Lepš 2014).

2.6. Vertical zooplankton distribution

We calculated the weighted mean depth (WMD) for selected taxa to determine seasonal changes in taxa vertical distribution. The mean depth (Zm) and the standard deviation of the frequency distribution with depth (Zs) were calculated following Daase et al. (2016):

$$Zm = \sum_{j-1}^{n} w_j z_j \quad (1)$$

$$Zs = \sqrt{\sum_{j=1}^{n} w_j z_m^2 - Z_m^2} \quad (2)$$

$$w_j = \frac{d_j f_j}{\sum_{j=1}^{n} d_j f_j} \quad (3)$$

where n is the number of depth intervals; w_j is the relative abundance within depth interval *j*; z_j is the mid depth (m) of sample interval *j*; d_j = lower depth – upper depth (m) of sample interval *j*; f_j is the density of individuals (ind. m^{-3}) in depth interval *j*. The WMD (Zm) indicates the mean depth at which the majority of the population of a given taxa is located, while its standard deviation (Zs) is a proxy for the extent of the vertical distribution. Small Zs indicate that organisms were concentrated at a certain depth and large Zs that they were distributed over a larger depth range. Due to cruise logistics, sampling was done at different times of day and potential DVM effects were not included here, but a comparison of the WMD vs. time of day did not yield a correlation.

2.7. Zooplankton diversity

The zooplankton diversity at different stations and in different seasons was evaluated based on Shannon diversity index considering the number of taxa (richness) and their relative abundance (evenness) in respective communities.

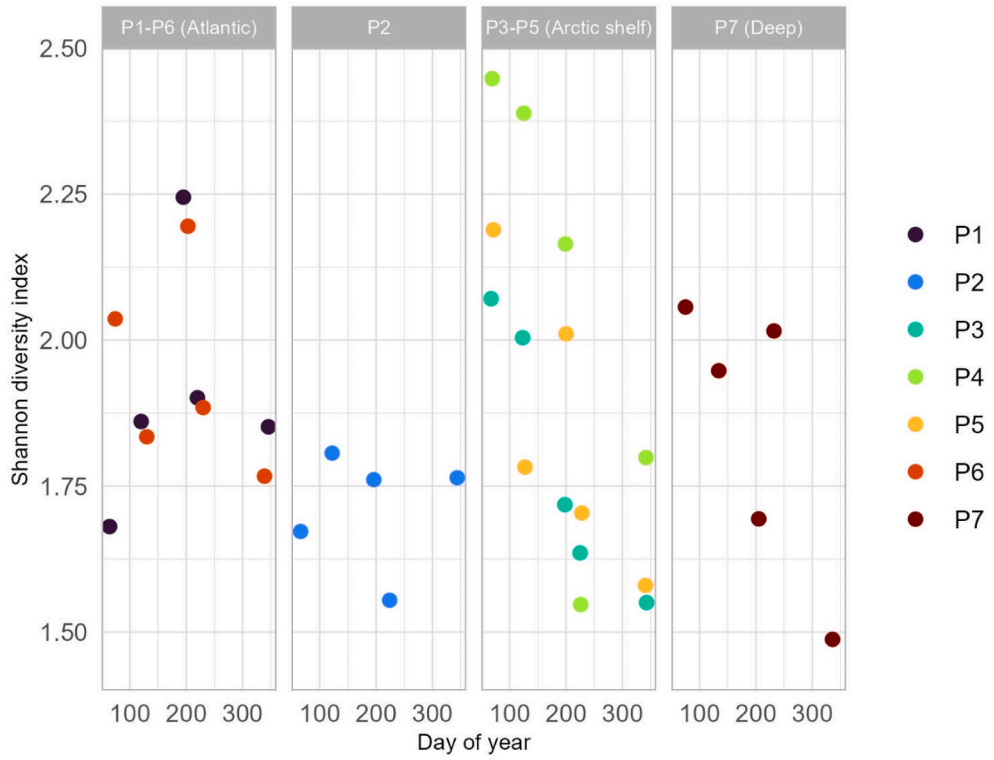

Fig. 3. Shannon diversity index for the mesozooplankton for the southern and northern Atlantic inflow areas (P1 and P6), the Atlantic shelf (P2), Arctic shelf (P3, P4 and P5) and the Arctic Ocean deep area (P7).

$$H = \sum [(p_i)]^* ln(p_i) \quad (4)$$

$$p_i = \frac{n}{N} \quad (5)$$

Where p_i is the proportion of individuals of the i^{th} taxa in a community, n is the number of individuals of each taxa and N is the total number of individuals of all taxa in a community, at a given station and season.

3. Results

3.1. Water mass distribution across seasons

The sampled transect stretched from south of the Polar Front (P1) across the northern Barents Sea shelf (P2-P5), crossing the continental slope (P6) into the deep Arctic Ocean (P7) (Fig. 1A). Station P1 was dominated by warm (T > 0° C) and salty (S > 34.9) modified Atlantic Water (MAW) that had entered the Barents Sea from the south (Fig. 2, Table 1). During summer (July and August) there was a fresher and warmer surface layer of warm Polar Water (wPW; T > 0 °C, S < 34.9) at P1 that was also present at stations P2-P5 in December. The top 200 m of the northern shelf stations P2-P5 were dominated by Polar Water (PW; T < 0 °C, σ_θ < 27.97 kg m^{-3}) that was partly imported from the Nansen Basin and partly a result of the local interaction with sea ice resulting in cooling and the input of fresh meltwater. In July and August in 2019, below 200 m at the stations P2 to P5, there were cold and salty Arctic Intermediate Water (AIW) and Central Barents Sea Dense Water (CBSDW; T < 0 °C, σ_θ > 27.97 kg m^{-3}) present, which was a result of sea-ice formation and deep mixing in winter, while in March, May and July 2021 wPW dominated below 200 m at P2-P5, which originated from strongly modified AW that had entered the shelf from the north. Mooring results indicate that the AW inflow from the north onto the Barents Sea continental shelf strengthens in winter (Lundesgaard et al., 2022), but also that the year 2019 was colder and had a larger sea-ice cover than winter 2020/21 (van England et al., 2023). Water masses at the continental shelf stations P2-P5 thus show signs of both seasonal and interannual variability. At the shelf break and deep ocean stations P6 and P7, the hydrography of the upper ocean and particularly the position of the AW core above 600 m generally followed the seasonal signal identified from mooring observation by Renner et al. (2018). Here a warmer, saltier, and less modified AW core was found in August and December 2019 compared to March and May 2021, whereas July 2021 was in the transition between the two states. The deep ocean below 600 m at P6 and P7 was filled with cold and salty AIW during all seasons.

3.2. Regional biodiversity

A closer look at zooplankton biomass classified by zoogeographical preferences shows a summer-peak (July and August) in the south and a late autumn-peak (December) in the north for advected Atlantic zooplankton (Fig. 1B). On the shelf, Arctic species dominated year-round with relatively high and stable biomass at the deepest shelf station P4. The high biomass of Atlantic species in late autumn (December) was mainly due to one copepod species, *Calanus finmarchicus,* which had particularly high biomass in the upper 50 m.

In total 74 zooplankton taxa were identified of which the majority were copepods (31 taxa), followed by Cnidaria (10 taxa). A clear seasonal trend in the Shannon diversity index was apparent on the shelf, with the highest diversity, especially at the deepest shelf station P4 in April and May, followed by a distinct decrease in diversity from May to December (Fig. 3). In contrast, the highest species diversity was in summer (July) in the core Atlantic inflow regions (P1 and P6). Station P2 separated from the other shelf stations with relatively low biodiversity throughout all seasons. The deep station P7 showed a similar trend as the Arctic shelf station, with a decrease in diversity over the season but with relatively high diversity in August 2019.

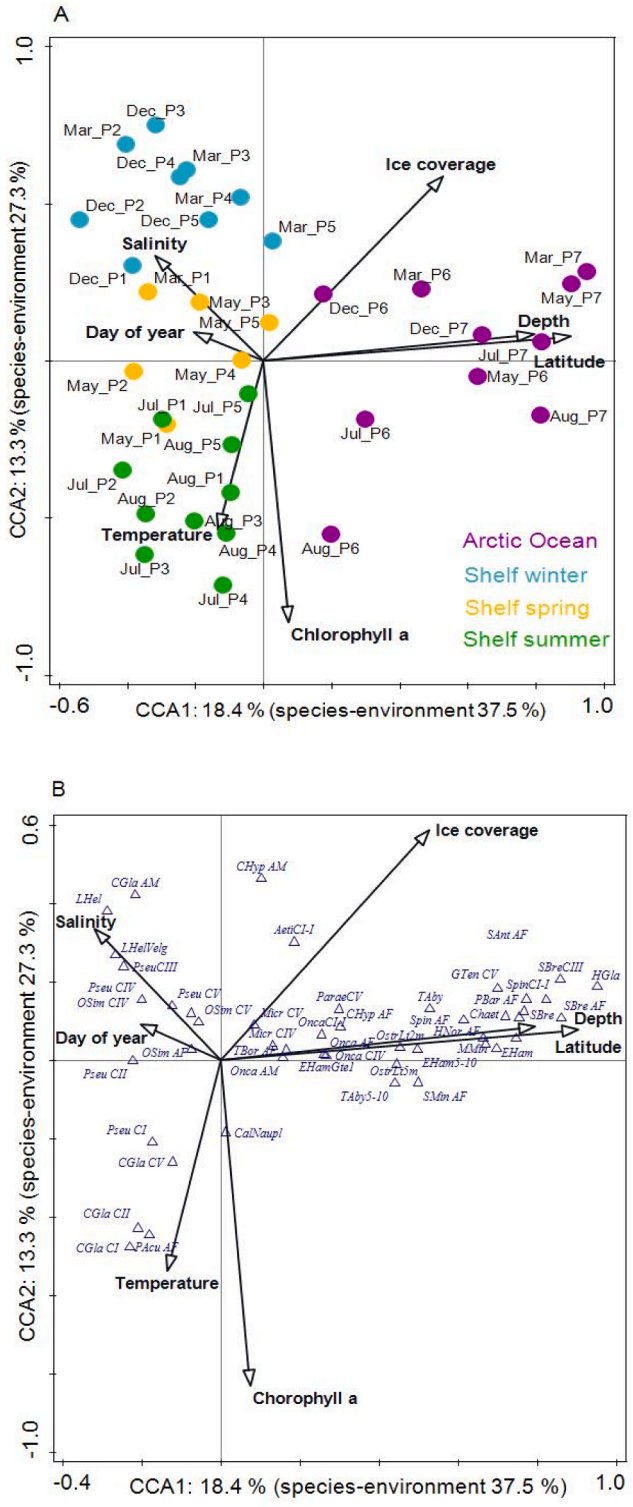

Fig. 4. The CCA of the total mesozooplankton community and environmental variables for all stations and all months. A) Biplot of samples and environmental variables where the groups of samples are displayed in different colours. The environmental variables, selected by a forward selection (see Table 3), are shown as arrows. B) Scatterplot of species occurrence at all depths, stations and seasons. Abbreviation following this pattern, e.g., *Calanus glacialis* CIII = CGlaCIII, see Supplementary table 1 for a full list of species names.

Table 2
Summary of Canonical Correspondence Analysis (CCA, where the total variation is 0.777).

	Eigenvalues	Explained variation (cumulative)	Pseudo-canonical correlation	Explained fitted variation (cumulative)
Axis 1	0.1427	18.37	0.9579	37.49
Axis 2	0.1039	31.74	0.8964	64.79
Axis 3	0.0530	38.57	0.8870	78.72
Axis 4	0.0323	42.72	0.8728	87.20

Table 3
Result of forward selection of explanatory variables in the CCA. The selected explanatory variables account for 49.2% of the variation in the zooplankton abundance data.

Explanatory variable	Explained %	Contributed %	p-value
Bottom depth (m)	15.6	31.8	0.002
Chlorophyll *a* (mg m^{-2}), upper 50 m	10.2	20.7	0.002
Latitude	5.6	11.4	0.002
Ice coverage (%)	5.2	10.5	0.004
Temperature mean, upper 50 m	5.0	10.2	0.010
Day of the year	4.4	8.9	0.002
Salinity mean, upper 50 m	3.2	6.5	0.024
Total	49.2	100	

3.3. Seasonal changes in zooplankton communities

The Canonical Correspondence Analysis (CCA) performed on the species abundance, considering developmental stages and size groups in total 192 unique taxa, revealed two clear gradients in zooplankton community composition. The first gradient correlated with a depth gradient from the shelf to the deep Arctic Ocean, which can also be described as a geographic gradient from south to north (CCA1, 18.4%). The second gradient reflected a seasonal change in environmental variables throughout the yearly life cycle, from autumn to winter, spring and summer (CCA 2, 13.3% (Fig. 4, Tables 2 and 3). The seasonal pattern was best explained by variability in chlorophyll *a* biomass and temperature in the upper 50 m as proxies (Table 3). Close to half (49.2%) of the mesozooplankton variability could be explained by the following seven environmental variables, which were (in order of their importance): bottom depth (15.6%), chlorophyll *a* in the upper 50 m (10.2%), latitude (5.6%), ice coverage (5.2%), temperature in the upper 50 m (5.0%), day of the year (4.4%), and salinity in the upper 50 m (3.2%) (Table 3). Zooplankton on the slope of the deep Arctic Ocean at stations P6 and P7 differed the most from that in the other study areas due to the presence of bathypelagic copepods such as *Paraeuchaeta* spp., *Scaphocalanus brevicornis*, *Scaphocalanus magnus, Spinocalanus* spp., *Gaetanus brevispinus* and *Heterorhabdus norvegicus.* The separation of zooplankton between seasons along CCA 2 was mainly due to the different ontogenetic developmental stages in copepods. In winter, the presence of males of *C. glacialis* and *C. hyperboreus*, combined with high abundance of *Limacina helicina* veligers, particularly at P4, was a distinct feature of the shelf winter community. However, in May, Atlantic advection did not reach the shelf further north than this southern P1 station. In May, the zooplankton at station P1 resembled that present at other shelf-stations in summer (July-August), with a significant proportion of younger life stages that are brought to the shelf with Atlantic waters. In summer (July and August), high abundances of copepod nauplii and younger developmental stages (CI and CII) of *C. glacialis* and *Pseudocalanus* spp. as well as of meroplankton were characteristic at P1 and for all shelf stations.

A hierarchical cluster analysis (Supplementary Fig. 1 and

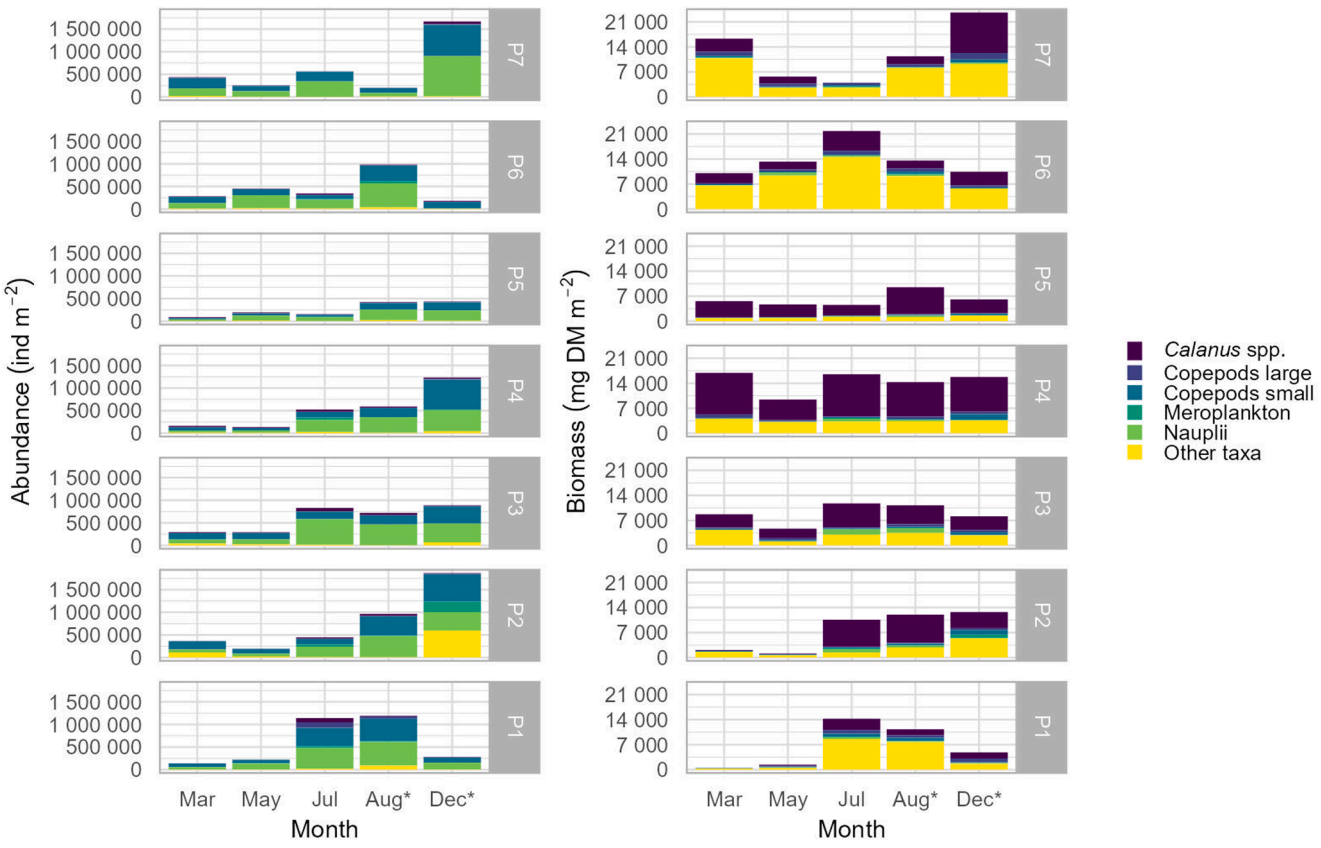

Fig. 5. Abundance (ind. m^{-2}) and biomass (mg DM m^{-2}) of all mesozooplankton taxa collected with MultiNet 64 μm and 180 μm at all stations (P1-P7) during all seasons (March, May, July, August and December).

Supplementary Table 2) showed similar community differences as the CCA (Fig. 4) with a distinct division between shelf stations (P1-P5) and slope/deep Arctic Ocean stations (P6 and P7). Further, it showed that station P1 dominated by modified Atlantic water (mAW) was somewhat different from the other shelf stations dominated by Polar Water (PW), except in March when station P1 comprised a mixture of PW and mAW. Four distinct zooplankton communities were identified (SIMPER, $p < 0.1$, $R = 0.719$): 1) A winter-spring PW shelf community that represented zooplankton found at stations P2-P5 in December, March and May, and that found at P1 in March (67.4% similarity, SIMPER); 2) A summer-autumn PW shelf community including zooplankton from P2-P5 in July and August (74.6% similarity, SIMPER), 3) A mAW community which could be further divided into a Winter (P1; December and May) and Summer mAW (P1; July and August) communities, but these were not significantly different and thus pooled into one mAW shelf community (59.3% similarity, SIMPER). The Arctic Ocean slope (P6) and basin (P7) zooplankton did not show distinct seasonal pattern and they were pooled into one (4) Arctic Ocean community (67.4% similarity SIMPER). Cyclopoida nauplii, small cosmopolitan copepods such as *Oithona similis* and *Pseudocalanus* spp. were present ubiquitously and in high numbers (>100,000 ind. m^{-2}; Supplementary Table 3) everywhere, year-round, and contributed significantly to the similarity across all stations according to ANOSIM (Supplementary Table 2). In contrast, *Calanus glacialis* and *L. helicina* contributed to the difference between the Shelf and Arctic Ocean communities as both species were most abundant on the shelf. The zooplankton at P1 differed from that at other stations on the shelf in the high abundance of juvenile stages of *O. similis* CI-CIV, *Microcalanus* spp. CI-CV and *Pseudocalanus* spp. CI-CII, combined with higher abundances of *Microsetella norvegica* and *Metridia longa*. The difference in these characteristics may have resulted, in part, from the seasonal cycle of development which have different time course at the southern stations than further north on the shelf and the Arctic Ocean.

The overall abundance and biomass of zooplankton varied with the seasons (Fig. 4 and Supplementary Tables 3 and 4). At the southernmost station P1, the number of zooplankton peaked in July and August with more than 1 mill. ind. m^{-2}, decreased at the beginning of winter and reached a minimum in spring with less than 150,000 ind. m^{-2} (Fig. 5). High abundance in summer was associated with high biomass, with a maximum of 14.3 g m^{-2} in July and with still high value of 11.3 g m^{-2} in August, which decreased to minimum ~ 1 g m^{-2} in spring (March and May). Further north, at stations P2-P5, zooplankton abundance increased over time and peaked in December, albeit at different levels. The highest abundance at the end of the annual cycle was observed at P2 (1.8 mill. ind. m^{-2}) and the smallest at P5 at the shallow centre of the shelf (400,000 ind. m^{-2}). The total zooplankton biomass varied seasonally at shelf stations in different ways. While the biomass at P2 increased from May to December, less seasonal fluctuations were recorded at P3, P4 and P5 (Fig. 5). Different seasonal patterns in zooplankton abundance and biomass were apparent on the northern shelf and slope of the Barents Sea, at the fringe of the Arctic Ocean where the abundances were high in August at P6 (approx. 1 mill. ind. m^{-2}) and in December at P7 (1.6 mill. ind. m^{-2}). The biomass, on the other hand, peaked in July at P6 (21.9 g m^{-2}) and in December (23.6 g m^{-2}) at P7.

The seasonal increases in abundance and biomass were the most pronounced at P1, P6, and P7, the stations with the strongest influx of Atlantic water. In contrast, the shelf stations north of the Polar Front, P3, P4, and P5 showed less variations in abundance and biomass throughout the seasons. The strong seasonal signal at P1 was due to an increase in species such as *Oithona similis* (from 50,000 ind. m^{-2} in May to 330,000 ind. m^{-2} in August), *Metridia longa* (from 170 ind. m^{-2} in March to 120,000 ind. m^{-2} in July), and *Calanus finmarchicus* (from 130 ind. m^{-2} in March to 79,000 ind. m^{-2} in July). The increases in abundance and biomass seen at P6 and P7 in August and December were also due to a doubling in numbers of *C. finmarchicus* and *Oithona similis* as well as in

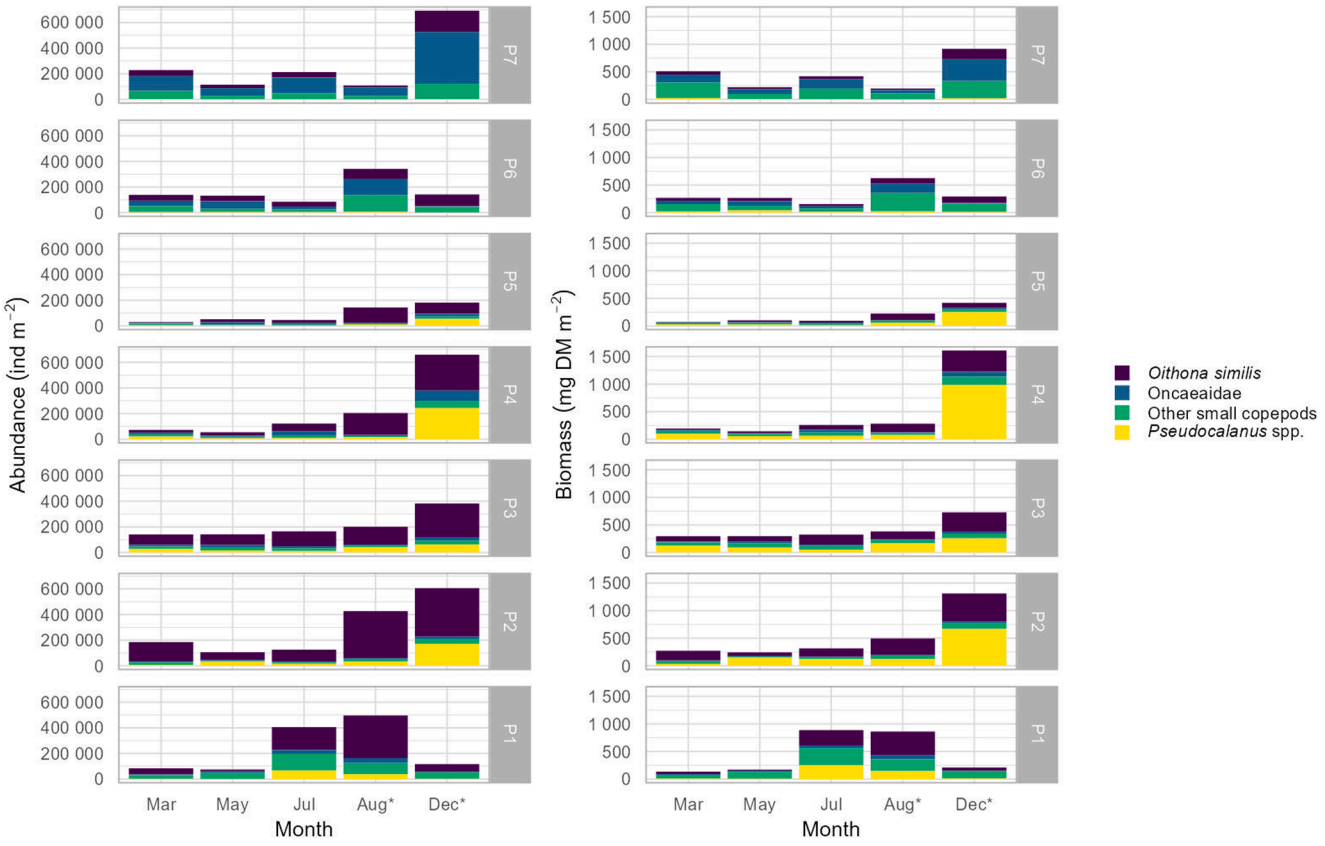

Fig. 6. Abundance (ind. m^{-2}) and biomass (mg DM m^{-2}) of small copepods at all stations (P1-P7) during all seasons (March, May, July, August and December).

oncaeids, represented in the majority by *Triconia borealis*. This last species was not observed at P1. The increase in total mesozooplankton abundance was due to increases in the abundance of many taxa, copepods, both small and larger, as well as meroplankton while the increase in biomass was mainly driven by the rise in numbers and ontogenetic development (emergence of older copepodids) of *C. finmarchicus* at P1, P6, and P7 and of *Calanus glacialis* at P3-P5.

Meroplankton biomass increased on average 30 times from March to July, all stations included, with Echinodermata, Polychaeta and Bivalvia larvae contributing the most to this. Other meroplankton taxa contributed little to the increase in total biomass. The high biomass contribution of other taxa (e.g. 13.1 g m^{-2} at P6 in July) was due to appearance of amphipods such as *Themisto libellula* and *T. abyssorum*, chaetognaths such as *Parasagitta elegans* and *Eukrohnia hamata* or euphausiids *Thysanoessa* spp. Juvenile *Limacina helicina* contributed to the overall abundance (590,000 ind m^{-2}) and biomass (2.6 g m^{-2}) at P2 in December.

The small copepod species *Oithona similis*, *Pseudocalanus* spp., and onceids (predominantly *Triconia borealis*) were numerically dominant at all stations and in all seasons, but contributed less to the total biomass (Figs. 5, 6, Supplementary Tables 5, 6). However, there was a build-up in numbers and biomass of small copepods from summer to winter with the earliest peak of 500,000 ind. m^{-2} (and 890 mg m^{-2}) in August at P1, and with the peak observed later further north with abundance and biomass reaching 600,000 ind. m^{-2} (>1.0 g m^{-2}) in December at P2, P4 and P7 (Fig. 6). Interestingly, in the case of the small copepods, the seasonal course of changes at station P6 was similar to that at station P1, with a maximum of 0.6 g m^{-2} in August, although the extent of changes was less pronounced at P6.

Calanus spp. were the main contributor to biomass at all stations ranging from 0.02 g m^{-2} at P1 in March to 11.9 g m^{-2} at P4 in July. *Calanus finmarchicus* dominated both in numbers and biomass at P1, P6, and P7 and the species presence was strongly influenced by the inflow of Atlantic water with a marked increase at P1 in July (8000 ind. m^{-2}, 2.8 g m^{-2}) and at P6 (20,000 ind. m^{-2}, 3.0 g m^{-2}) and P7 (56,000 ind. m^{-2}, 9.6 g m^{-2}) in December (Fig. 7 and Supplementary Tables 7, 8).

Calanoid nauplii peaked at shelf stations in July and August (P3 and P4) (Fig. 8), suggesting intense seasonal population development following spring reproduction. Cyclopoid nauplii were present in high numbers at all stations and during all months with a peak at P7 in December.

Calanus glacialis dominated at the shelf stations north of the Polar Front (P3, P4, and P5). The biomass of *C. glacialis* at these stations ranged from 2.7 to 11.9 g m^{-2} (Fig. 7). The recruitment of young *C. glacialis* copepodid stages, CI, and CII appeared in July (Fig. 9). However, CI and CII were still relatively numerous at the shelf stations P2 (17,000 ind. m^{-2}), P3 (41,000 ind. m^{-2}), P4 (10,000 ind. m^{-2}) and P5 (3600 ind. m^{-2}) in August indicating that the reproduction at these stations could have started in June and continued over the summer while at P1 the reproduction occurred earlier as indicated by a peak in CI and CII (13,000 ind. m^{-2}) in July. *Calanus glacialis* was less abundant at P6 and P7. *C. glacialis* overwintered primarily as stages CIII and CIV in the entire study region. Adult females peaked at P4 in December (3800 ind. m^{-2}) and March (6000 ind. m^{-2}), while males peaked in at P2 December (4600 ind. m^{-2}) and was more or less absent (0–78 ind m^{-2}) at all stations in March.

Calanus finmarchicus occurred in the largest numbers at sites P1, P6 and P7 (Fig. 10). The highest abundance at station P1 was recorded in July, for young stages CI-CIII. Some young stages (CI) were also present at P6 while at P7 the increase in *C. finmarchicus* population occurred later in the season (December) and was mainly comprised of older life stages such as CIV and CV.

Metridia longa was the most abundant of the remaining larger non-*Calanus* copepods at all stations (Fig. 11 and Supplementary Tables 7, 8). The contribution of *M. longa* to zooplankton community at P1 in July was substantial (50,000 ind. m^{-2}), comprising primarily of young stages. *Paraeuchaeta* spp., which are large copepod, were also present

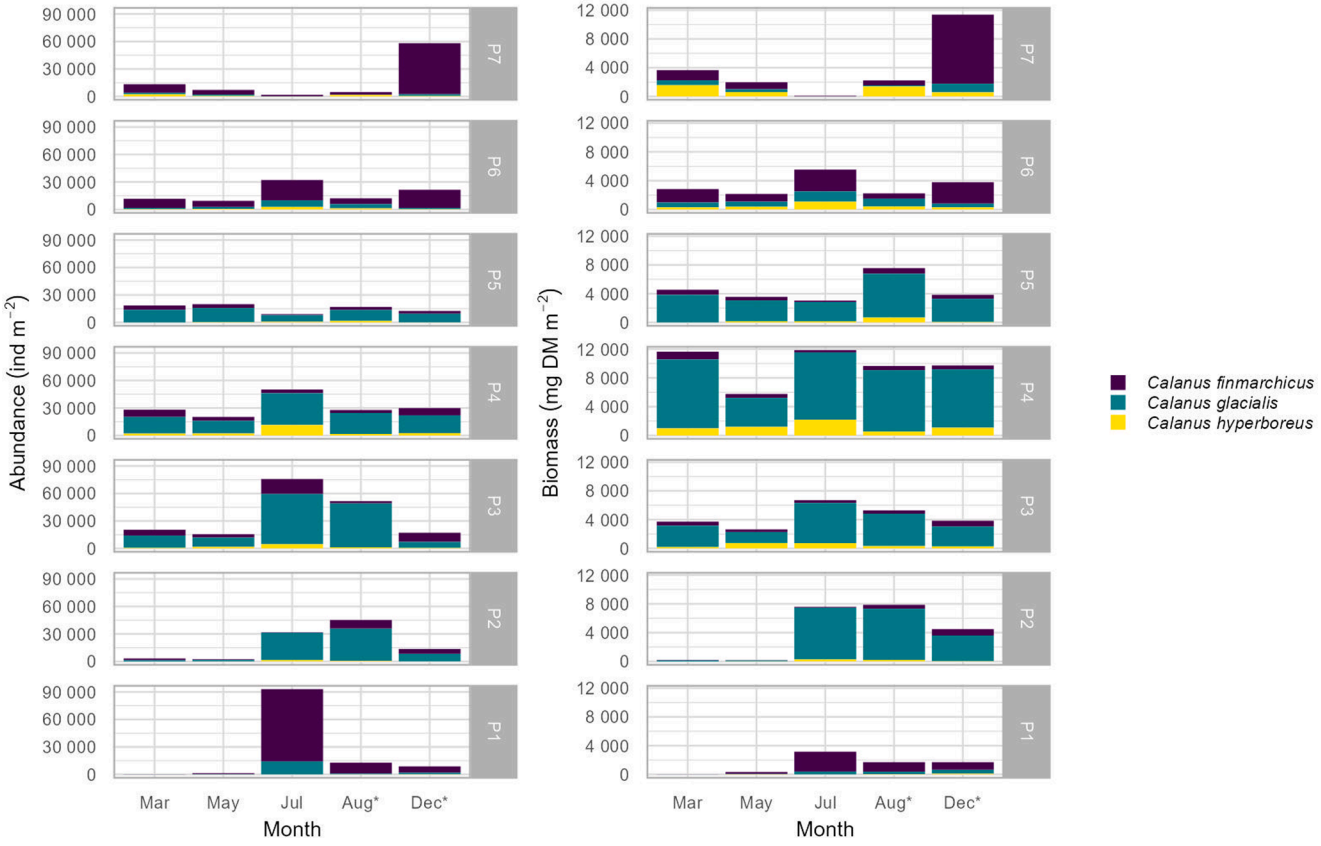

Fig. 7. Abundance (ind. m^{-2}) and biomass (mg DM m^{-2}) of all copepodid stages of *Calanus* spp. at all stations (P1-P7) during all seasons (March, May, July, August and December).

across all stations and increased in abundance northwards, with a peak in July at P6 (720 ind. m^{-2}). At the deep stations P6 and P7 large deep-water copepods such as *Scaphocalanus magnus*, *Heterorhabdus norvegicus,* and *Gaetanus tenuispinus* contributed to the biomass in the deeper layers. With the exception of a large increase in the abundance of juvenile *Metridia longa* at P1 in July, our data did not show a consistent pattern of changes in the abundance of larger copepods across seasons.

Meroplankton was occasionally present in high abundance and the huge increase in Bivalvia numbers at the shelf in December (100,000–200,000 ind. m^{-2}) masked any other trends (Fig. 12 and Supplementary Tables 9 and 10). At much lower abundance levels, however, Echinodermata larva increased at the shelf stations in July (7300–51,000 ind. m^{-2}), but only occurred in low numbers in winter (10 to 1100 ind. m^{-2}).

The group of other taxa comprised a wide range of zooplankton organism including larger specimens that were not sampled representatively with the MultiNet (Fig. 13 and Supplementary Tables 11 and 12). *Limacina helicina* was present at all the shelf stations during all seasons with numerous juveniles at station P2 in December (590,000 ind. m^{-2}). *Fritillaria borealis* and *Oikopleura* spp. were important at several stations in July and August, with record abundance of 52,000 ind. m^{-2} and 7500 ind. m^{-2}, respectively.

3.4. Seasonal change in depth distribution

The weighted mean depth (WMD) calculated for copepod biomass revealed that all species were relatively evenly distributed throughout the water column during all seasons, but with slightly shallower distribution in July except at stations P1 and P6 (Fig. 14). The most pronounced shallowing of the bulk biomass was seen at the deep Arctic Ocean station (P7). The two predominantly herbivore species *Calanus glacialis* and *Calanus finmarchicus*, which constituted the bulk of the biomass at, respectively, P2-P5 (*C. glacialis*) and P1 and P6, showed similar seasonal WMD pattern at most stations. Both species had the shallowest distribution in March followed by another relatively shallow WMD in July, except at station P6. The relatively large variation in WMD shows that a large fraction of the population was distributed throughout the water column with no distinct optimum depth.

4. Discussion

4.1. Regional differences - inflow of Atlantic water

Zooplankton abundance, biomass and community structure are strongly related to hydrography (Blachowiak-Samolyk et al., 2008b; Daase and Eiane, 2007; Søreide et al., 2003). In the Barents Sea and Arctic Ocean, one of the main features affecting the zooplankton is the inflow of Atlantic water (e.g. Edvardsen et al., 2003; Aarflot et al., 2018). We found that the inflow of Atlantic water strongly impacted the seasonality of the zooplankton communities south of the Polar Front (P1) and along the slope north of Svalbard (P6 and P7). The stations were positioned within the Atlantic current and had high abundances of Atlantic and cosmopolitan affiliates such as *C. finmarchicus* and *Metridia longa*, especially during summer and autumn following periods of increased Atlantic water inflow. At the shelf stations (P2-P5), an Arctic community dominated by *C. glacialis, Pseudocalanus* spp. and *Limacina helicina* was found and it was the presence of young copepodid stages and meroplankton larvae in summer that separated the zooplankton communities in summer and winter communities at these stations. In the course of annual seasonal changes, the pulse in the inflow of Atlantic species occurred earlier in the season in the southern end of our study section (P1) than along the northern slope (P6). In the south, Atlantic water enters through the Barents Sea Opening in quantities that are linked to the local atmospheric pressure fields (Ingvaldsen et al., 2002;

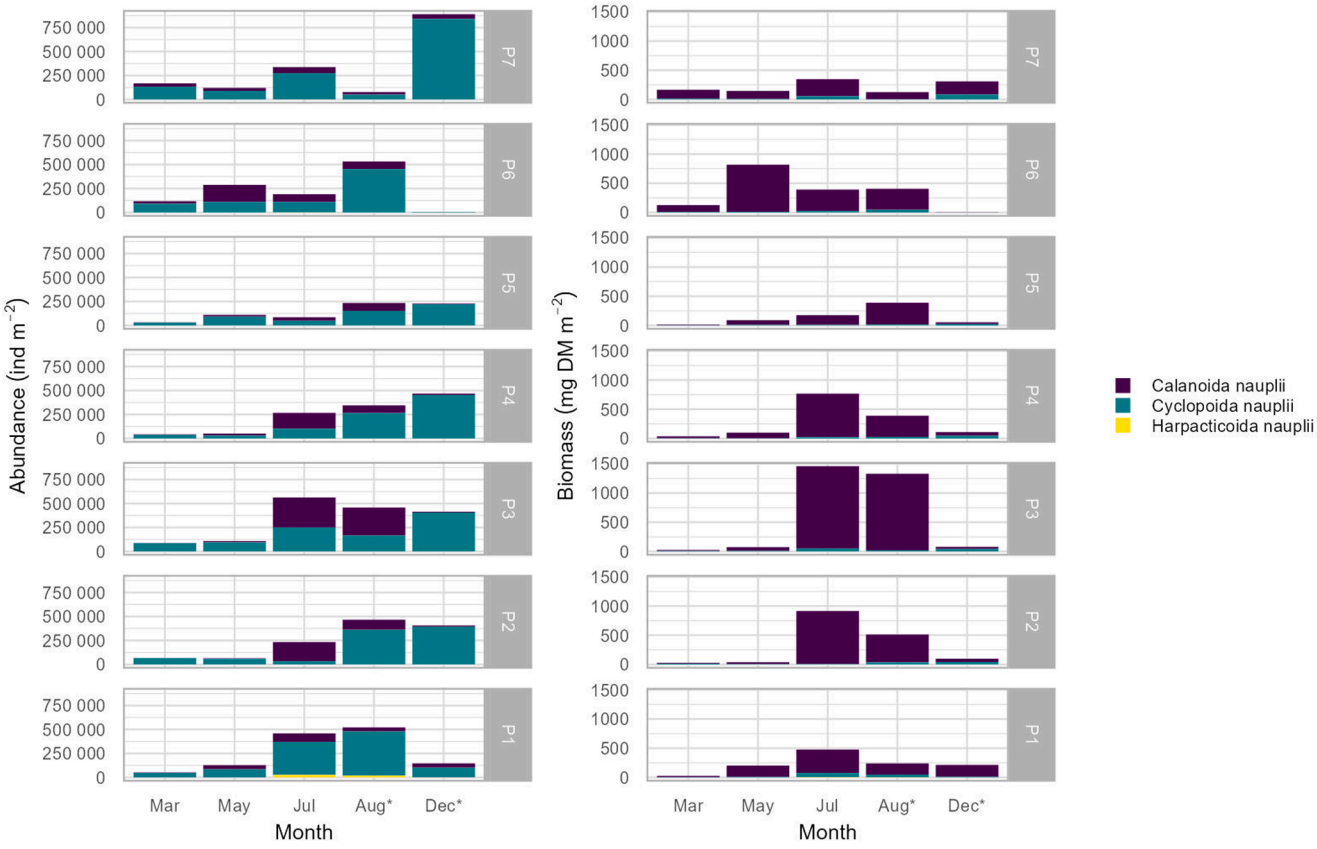

Fig. 8. Abundance (ind. m^{-2}) and biomass (mg DM m^{-2}) of copepod nauplii at all stations (P1-P7) during all seasons (March, May, July, August and December).

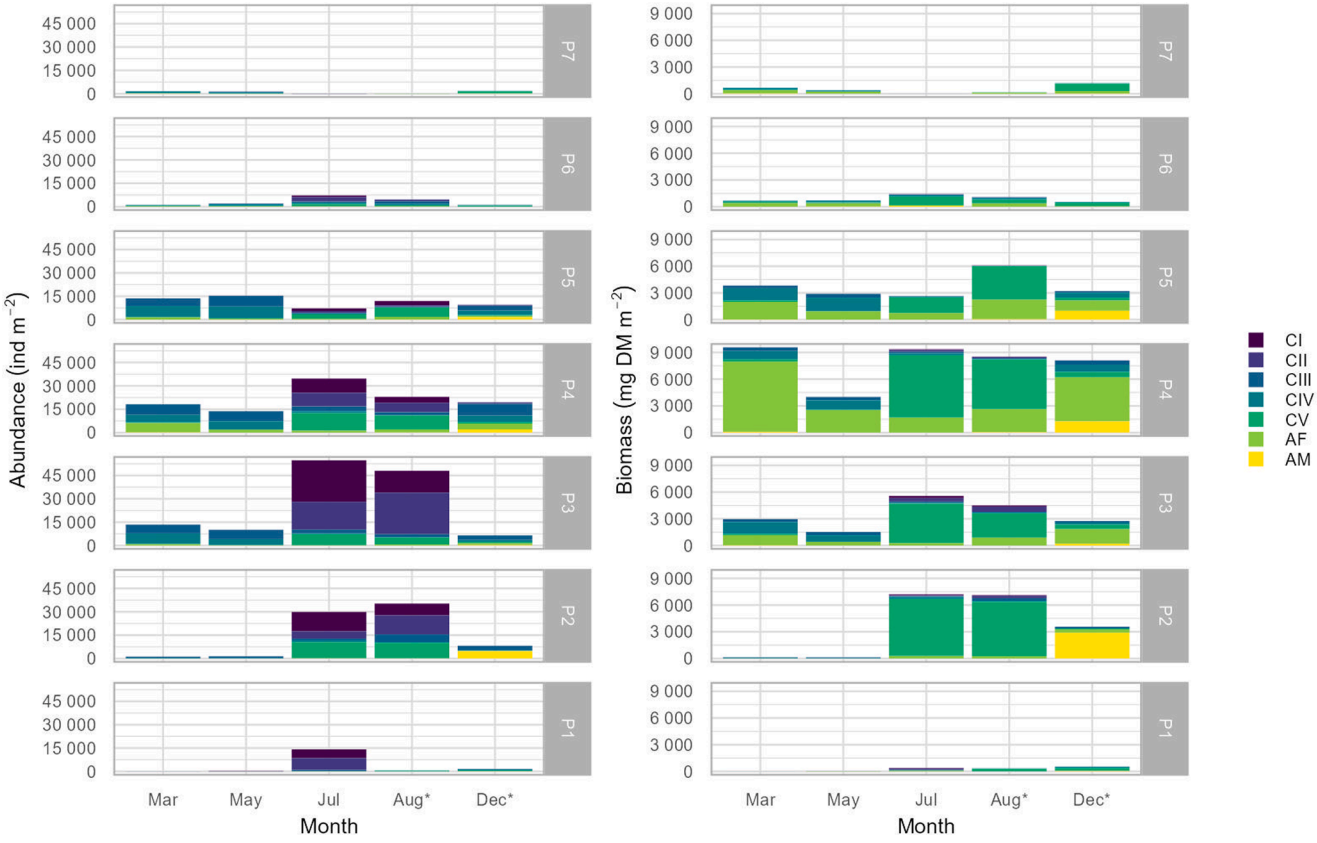

Fig. 9. Abundance (ind. m^{-2}) and biomass (mg DM m^{-2}) of all *Calanus glacialis* at all stations (P1-P7) during all seasons (March, May, July, August and December).

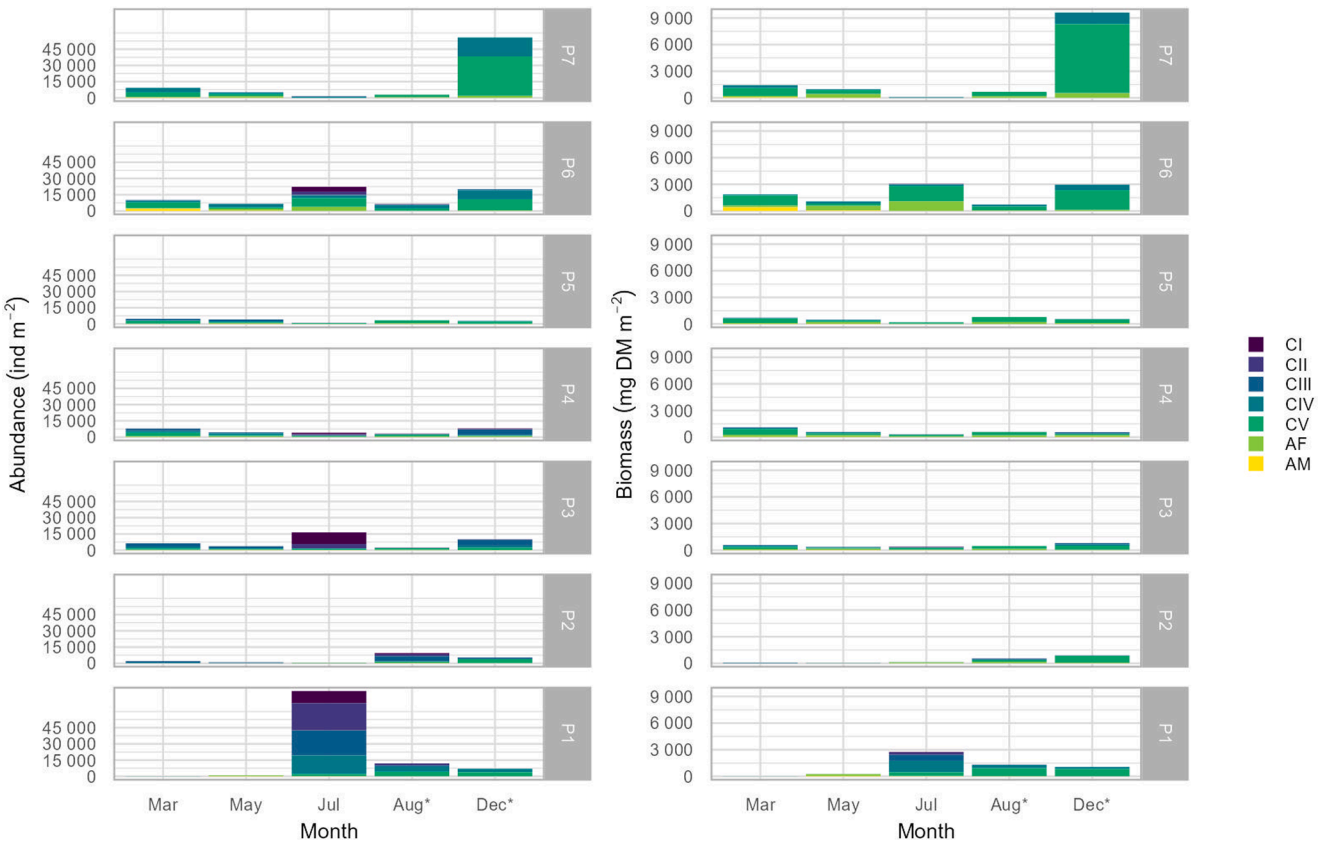

Fig. 10. Abundance (ind. m^{-2}) and biomass (mg DM m^{-2}) of all *Calanus finmarchicus* at all stations (P1-P7) during all seasons (March, May, July, August and December).

Polyakov et al., 2023). Ingvaldsen et al. (2002) did not find a distinct seasonal pattern in the inflow of Atlantic water through the Barents Sea Opening but observed a widening of the inflow area in summer. In the north, the Atlantic Water Boundary Current transports water along the coast of Svalbard into the Nansen Basin (Renner et al., 2018). The increased abundance of Atlantic zooplankton species found in the north results from the same "pulse of inflow from the south" as observed south of the Polar Front in summer, although delayed. Results from modelling studies suggest that mesozooplankton on the shelf north of Svalbard may derive from populations along the North Norwegian and western Barents Sea shelf break regions (Wassmann et al., 2019). Assuming an average advection speed of 0.2 m s^{-1}, it would take two months for the water mass to travel from the southern tip of Svalbard along the shelf break to the area of station P6. The pulse of increased abundance and biomass of Atlantic species will therefore occur later in the season at P6 and P7 than at P1, as observed in our study. The observed annual temperature maximum north of Svalbard at 81° 30'N, 31° 00'E in mid-November indicated that the strongest effect of the Atlantic inflow is emerging in the northern reaches of the Atlantic water flow in late autumn (Ivanov et al., 2009), which agrees with our observations. Basedow et al. (2018) quantified the inflow of zooplankton biomass through the Fram Strait in January, May, and August and found the highest biomass in August and January, which also supports of our finding of the highest biomass of Atlantic species during late autumn.

The highest zooplankton diversity was recorded at the deepest shelf station P4, indicating that the zooplankton advected either from north or south could be retained in this area since it is deeper than surrounding areas. The Atlantic stations P1 and P6 had the highest diversity in the summer as a result of the advection of Atlantic species. A similar but weaker tendency was also seen at station P7 further north, with a relatively high biodiversity in early August, slightly delayed compared to that at station P6 in the core Atlantic inflow along the northern slope. Atlantic species were also present at shelf stations P2-P5, but less copious and without the strong seasonal pulses of increased abundance and biomass as in the inflow areas. The Polar Front, which to a large extent is defined by topographic structures in this area, may serve as a barrier for the northward transport of zooplankton (Blachowiak-Samolyk et al., 2008a,b; Søreide et al., 2003). The two possible northern gateways of Atlantic water to the Barents Sea, the Kvitøya Trough and Franz Victoria Trough (Lundesgaard et al., 2022) probably do not allow the entry of large amounts of water and large numbers of Atlantic species. Thus, the zooplankton community on the shelf north of the Polar Front remains relatively consistent over time.

The seasonal difference in the zooplankton community structure on the shelf was mainly due to ontogenetic development of copepods with the presence of copepod females and males in winter and young stages such as CI and CII during summer. The emergence of meroplankton, such as Echinodermata larvae, in summer, was an indication of seasonality in the development of local benthic organisms and was, thus, an expected feature of zooplankton dynamics for shelf areas (Descôteaux et al., 2021).

4.2. Seasonal changes in total abundance and biomass

The large and predominantly herbivorous copepods such as *Calanus* spp. were major contributors to the total mesozooplankton biomass along the transect, with *C. finmarchicus* being most abundant in the inflow areas (P1, P6 and P7) and *C. glacialis* most abundant in the shelf area (P2-P5). At P1 and P2, the biomass of *Calanus* spp. increased by one order of magnitude from March to July and the increase was even larger at P7 but occurred first in December. On the shelf, the seasonal differences of *Calanus* spp. were less pronounced. *Metridia longa* also contributed to the zooplankton biomass at all stations, especially in the south during summer. Zooplankton biomass in the Barents Sea is

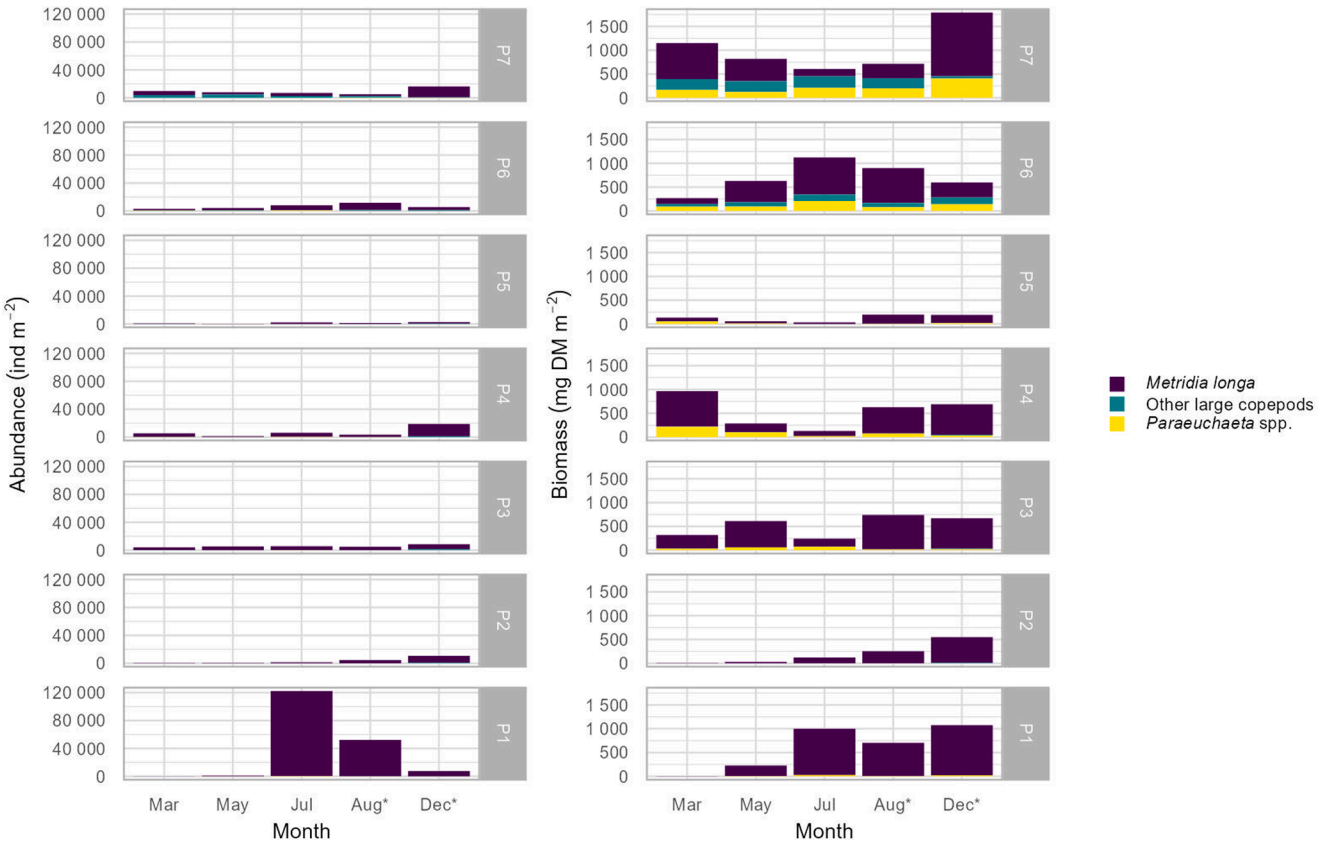

Fig. 11. Abundance (ind. m^{-2}) and biomass (mg DM m^{-2}) of other large copepods at all stations (P1-P7) during all seasons (March, May, July, August and December).

controlled by both physical conditions such as advection, temperature, and primary production (bottom-up, Dalpadado et al., 2014, 2020) and predation of fish, especially capelin (*Mallotus villosus*) top-down; The relative contribution of bottom-up versus top-down processes in controlling the zooplankton biomass was not addressed in our study, but the zooplankton biomass was largely affected by advection in the inflow areas as well as the bottom typography defining the main current pattern in the area. Hence, the seasonal variations in biomass were greater in the inflow areas than on the shelf mainly due to variable influx of *C. finmarchicus*. At the shelf stations, the seasonal variations were less due to the stable presence of *C. glacialis.* In contrast to the distinct seasonal increase in biomass that we observed from winter to summer, a study from 1998 to 99 showed no considerable change in zooplankton biomass between March, May, and July but with station-to-station variation (Arashkevich et al. 2002). The difference between what was observed in this area in 1998–1999 and what we observed in 2019–2021 indicates an increased seasonality in zooplankton biomass in the southern Barents Seas during this period.

The estimated annual net primary production (NPP) for the Barents Sea has more than doubled over the period 1998–2017 (Dalpadado et al., 2020). Such an increase in primary production would likely support larger zooplankton biomass. However, the increase in primary production has been less in the western Barents Sea than in the area further east in the Barents Sea (Castro de la Guardia et al., accepted). Based on satellite-derived chlorophyll *a*, Dalpadado et al. (2014) showed that phytoplankton bloom in the Barents Sea usually peaked in May, constituted about half of the annual primary production and comprised the basis for most of the zooplankton production. The total mesozooplankton biomass observed in our study in August (9.5–14.3 g DM m^{-2}) was slightly higher, but within the same range as that reported for the period 1998–2011 (5.4–7.9 g DM m^{-2}; Dalpadado et al., 2014) and for that reported in 1998–1999 (1–14 g DM m^{-2}, Arashkevich et al. 2002). The biomass of *Calanus* spp. showed the same tendency (1.7–9.8 g DM m^{-2} in the present study vs. 2.6–3.8 g DM m^{-2} in 1998–2010). This suggests that the total biomass of zooplankton has increased during the last decade (e.g. Aarflot et al., 2018; Gerland et al., 2023). However, interannual variability in total zooplankton biomass may be substantial (Dalpadado et al., 2020). Thus, obtaining reliable baselines and trends for zooplankton biomass are needed for future observations and assessments of climate change (Siwertsson et al., 2023).

The magnitude, timing, and duration of the spring bloom are important for mesozooplankton reproduction and development (Daase et al., 2013; Hop et al., 2021b). In 2021, the bloom started in May and continued throughout July with the highest chlorophyll *a* biomass standing stock at P1 and P6 in May and at P4 and P5 in August (P. Assmy pers. comm.). At the shelf area, the reproduction of *Calanus finmarchicus* and *C. glacialis* started in May, coinciding with the phytoplankton bloom, and it continued there throughout the summer. Such prolonged period of reproduction is also shown in models of *C. glacialis* population in the area (Aarflot et al., 2023) as well as in earlier studies of *C. finmarchicus*, *C. glacialis* and *C. hyperboreus* by Melle and Skjoldal (1998). The propagation of the bloom from south to north between May and July ensures a relatively long reproductive period for these key zooplankton species. This concurs with our observations of *Calanus* nauplii, which were abundant throughout the summer at the shelf area north of the Polar Front. With less sea ice, the seasonal bloom extent may expand northwards and also be manifested as autumn blooms in shelf seas (Ardyna et al., 2014; Renaut et al., 2018).

Several studies have shown that the Atlantic *C. finmarchicus* is moving northward into the Arctic Ocean (Aarflot et al., 2018; Wassmann et al., 2019; Ershova et al., 2021), but it is still under discussion whether this species will be able to reproduce and establish a stable population there. However, *C. finmarchicus* is likely successfully reproducing in the Fram Strait area (Tarling et al., 2022). In our study, we observed the

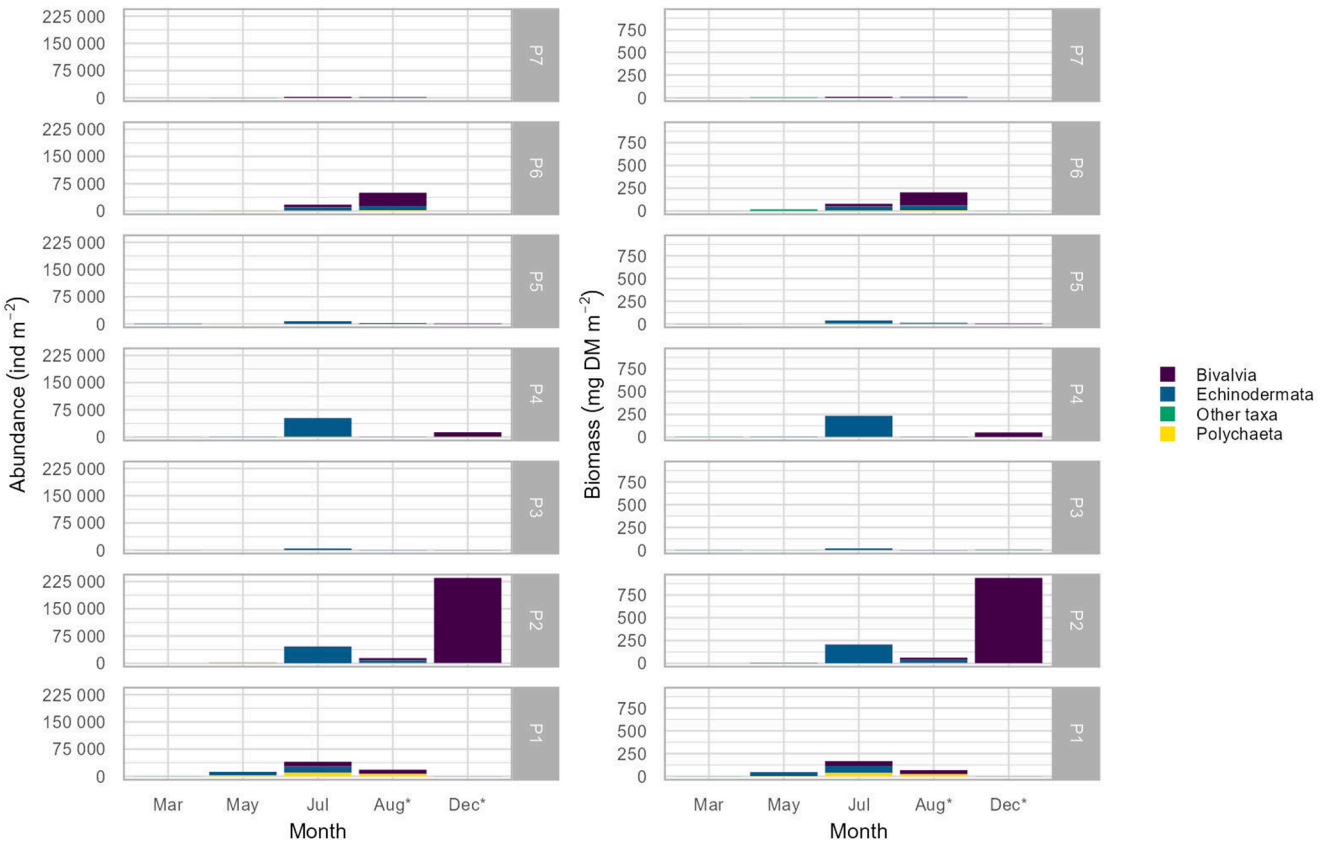

Fig. 12. Abundance (ind. m^{-2}) and biomass (mg DM m^{-2}) of meroplankton at all stations (P1-P7) during all seasons (March, May, July, August and December).

presence of *C. finmarchicus* all year round, in all seasons, both in the inflow areas and on the shelf. North of the Polar Front, the copepodid stages CIV and CV were the most numerous representatives of the species. The younger stages were only apparent in summer in the southern inflow area (P1). This is interpreted as evidence of successful reproduction and the emergence of the next generation in the Atlantic domain. We observed a small presence of females and males in the winter and spring also in the Arctic Ocean (P6 and P7), but the summer population of this species in these northern regions was modest, and high abundance and biomass were only recorded at the end of the annual cycle (December). This indicates, so far, that most of the *C. finmarchicus* found in inflow areas north of Svalbard do not reproduce successfully in Arctic water masses and are primarily advected in the Atlantic Water Boundary Current, which supports earlier findings by Hop et al. (2019).

4.3. Regional biodiversity

We observed higher taxonomic diversity of zooplankton on the shelf than in the inflow areas and the highest diversity was found at the shelf stations in winter. The seasonally decreasing diversity at the shelf stations may be explained by high abundance of *Calanus glacialis* and low diversity and abundance of meroplankton in winter. The diversity of zooplankton at the Atlantic inflow stations was high in summer but did not display a seasonal pattern. This could indicate that fewer zooplankton were transported northwards with the Atlantic Water current in winter or that our sampling potentially missed the main releases of benthic larvae in the region south of the Polar Front, which tend to be ephemeral.

At the northern slope and Arctic Ocean, the zooplankton community differed from the shelf-communities by the presence of deep-water Arctic copepod species, such as *Paraeuchaeta* spp., *Scaphocalanus brevicornis*, *Scaphocalanus magnus, Spinocalanus* spp., *Gaetanus brevispinus* and *Heterorhabdus norvegicus*, which is in accordance with previous studies (Kosobokova et al., 2011). These deep-sea species reproduce year-round and, thus, are independent of the spring bloom. Therefore, their presence in the water column and diversity, especially at deep stations, are less seasonally variable. The relatively high biodiversity at depth despite the homogeneous pelagic environment can be interpreted as the result of vertical partitioning of the habitat in order to reduce inter-specific competition (Laakmann et al., 2009).

4.4. Calanus glacialis

Calanus glacialis dominated the zooplankton community on the shelf. Both nauplii and young copepodids CI and CII of *C. glacialis* were abundant in July indicating that the reproduction likely started in May and continued during summer. A high proportion of females in winter and spring indicates that this species is ready for reproduction already at the beginning of the annual zooplankton development cycle. Therefore, the species may begin reproduction in spring or early summer, taking advantage of, depending on the circumstances, an ice algae bloom or a water column phytoplankton bloom, and may then actively continue to develop the new generation, exploiting phytoplankton in the water column, and microbial loop and microzooplankton until late summer. The presence of nauplii in July observed in our study is consistent with model simulations (Aarflot et al., 2023). On the other hand, the presence of CIII and CIV throughout the water column in winter and the lack of clear signs of diapause were unexpected. In the case of copepods of the genus *Calanus*, winter dormancy has been considered an essential part of the life cycle, for which the copepods prepare by accumulating lipid reserves in order to safely migrate to deep water for winter rest. *Calanus* in the Barents Sea has been reported to diapause at depth (Melle and Skjoldal, 1989), but recent studies (e.g. Kvile et al., 2019) have shown that Arctic *Calanus* has a broad depth distribution in winter, similar to our findings. Our failure to observe a diapausing population may be an

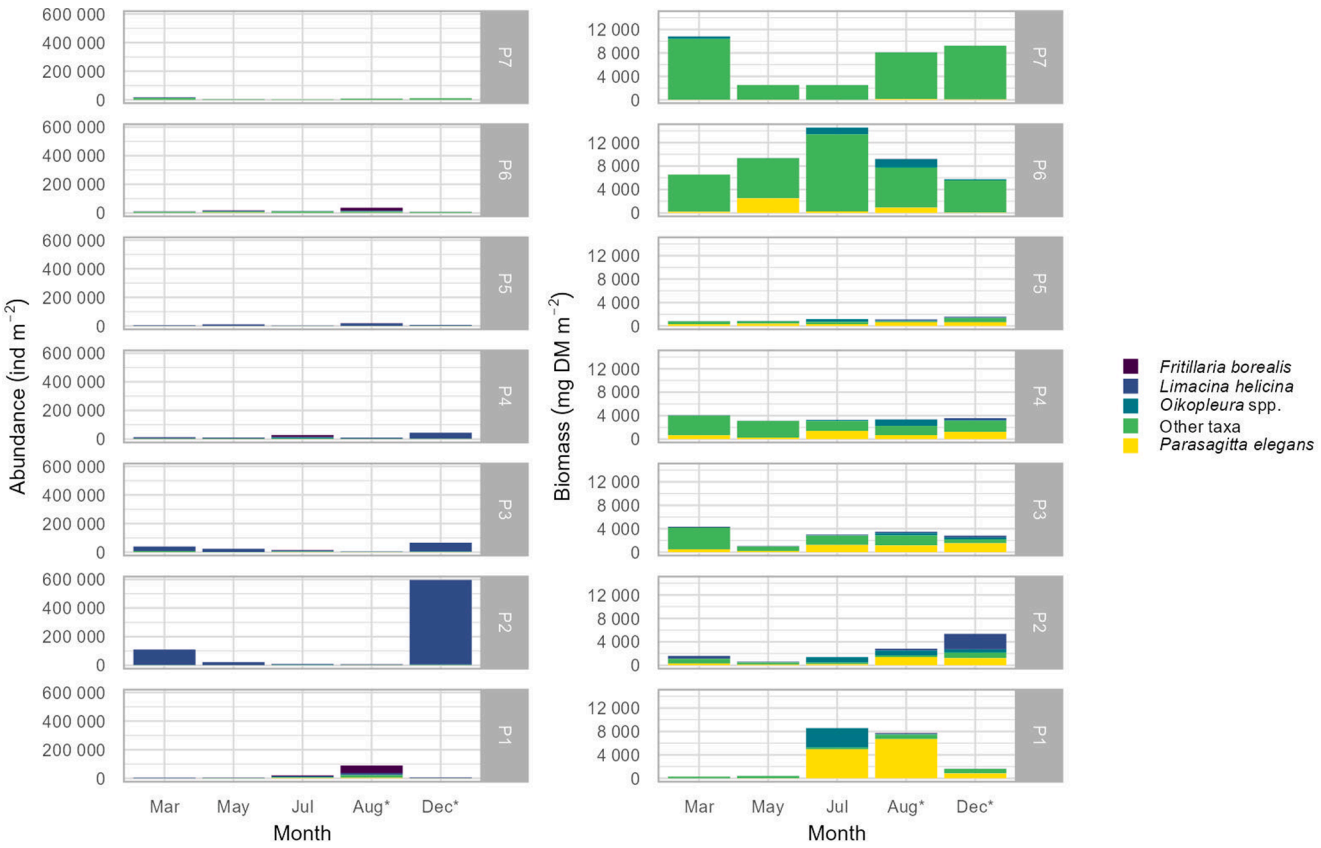

Fig. 13. Abundance (ind. m^{-2}) and biomass (mg DM m^{-2}) of other taxa than copepods and meroplankton at all stations (P1-P7) during all seasons (March, May, July, August and December).

artefact of not sampling as close to the bottom as possible due to concerns about damaging the net (the layer between 10 and 15 m above the bottom was typically not sampled) or it could have been the result of mixing of water masses by winter storms, bringing wintering copepods to the surface. The lack of ontogenetic migration could also be the result of the continued presence in the water column of a new generation of copepods, derived from females that bred later in the annual cycle and therefore remained in surface waters to feed rather than migrate to greater depths for diapause. DVM did not play a big role in your samples and a more thorough investigation of multiple samplings throughout a 24 period would be needed to elaborate on the DVM in this area during different seasons.

We found that the distribution of *C. finmarchicus* and *C. glacialis* overlapped little. While *C. finmarchicus* dominated in inflow areas in the south and along the slope north of Svalbard, *C. glacialis* was found mainly on the shelf area north of the Polar Front in accordance with model simulations (Aarflot et al., 2023). The peak in biomass for *C. glacialis* was found in our study in July and August, which differed from the result of model, in which the population peaked in May and June (Aarflot et al., 2023). This discrepancy could be explained by different rates of development in the model populations and the natural populations. It should be noted that our results are drawn from observations from two different annual cycles and the peak in biomass would likely differ from year to year due to the timing of the primary production and copepod reproduction.

4.5. Seasonal differences in depth distribution

Some copepod species, especially those considered to be mainly herbivorous, descend from the epipelagic zone in winter. However, we observed little seasonal difference in the depth distribution of herbivore copepods over the season, especially at the shelf stations. This might be because the Barents Sea shelf is shallow (mean depth 250 m) and with strong vertical mixing during winter due to storm events (Wassmann et al., 2006). In December we observed high numbers of herbivorous copepods, such as *C. finmarchicus*, in the surface water and also at the deep station P7. An active zooplankton community during winter has also been observed in previous studies (Barth-Jensen et al., 2022; Basedow et al., 2018; Blachowiak-Samolyk et al., 2015; Daase et al., 2014; Berge et al., 2015). However, the winter may cause large mortality in zooplankton (Daase et al., 2014; Daase and Søreide, 2021), which could be seen in our results, particularly for *C. finmarchicus* from December to May. We observed high numbers of *C. finmarchicus* CIV and CV in December at the deep Arctic Ocean station P7, but the lack of younger copepodid stages earlier in the season indicates that this species most likely does not reproduce this far north. There were some *C. finmarchicus* CI present at the shelf break station P6 in July which could indicate that *C. finmarchicus* have reproduced further south, in the Fram Strait (Tarling et al., 2022), and that offspring is carried with the currents northwards. We see signs of reproduction along the shelf break but not into the deep Arctic Ocean.

5. Summary

The Barents Sea is warming due to an increased inflow of Atlantic Water (Beszczynska-Möller et al., 2012), and zooplankton in the inflow areas south of the Polar Front and along the slope in the north were dominated by North Atlantic species such as *Calanus finmarchicus* and *Metridia longa*. The largest inflow seen as an expansion of the core Atlantic Water occurred during summer in the south and during late autumn–winter in the north. The mesozooplankton was seasonally variable in the Atlantic inflow areas, with large pulses in abundance and biomass during spring and autumn. On the shelf north of the polar front, zooplankton biomass was more stable throughout the year. Seasonal

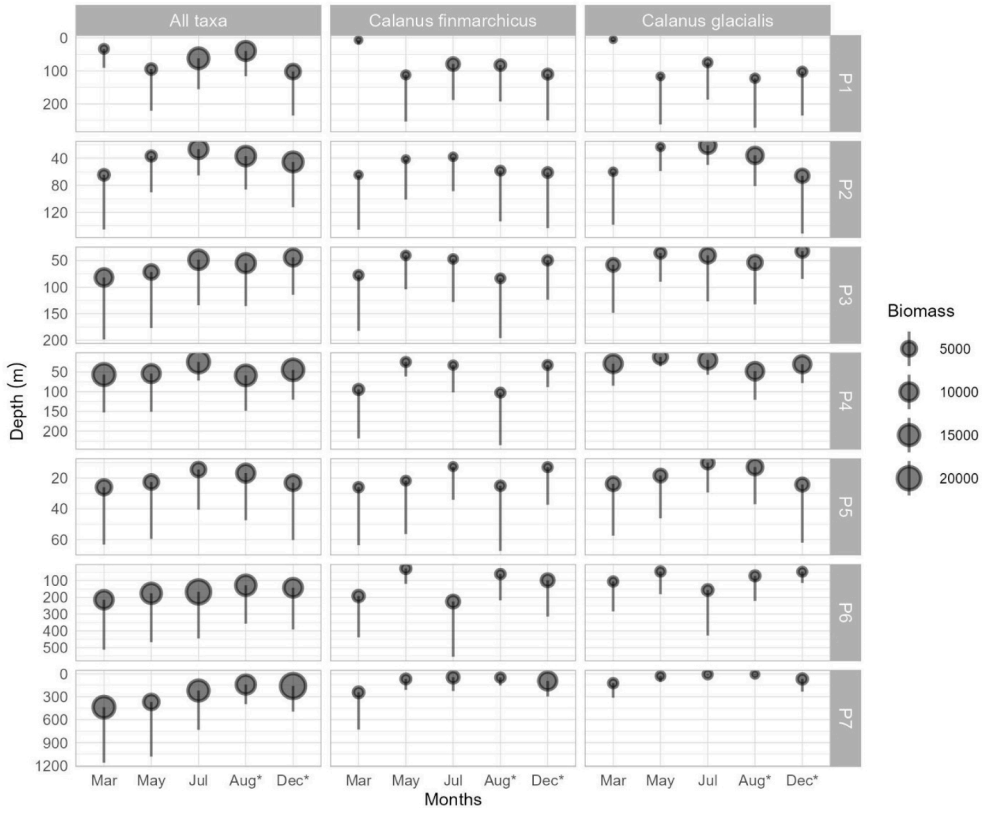

Fig. 14. Weighted Mean Depth of biomass for all taxa. Error bars indicate the spread (Z_s) of individuals over the water column, but only the downward spread is indicated. The bubble size reflects the mean abundance in the water column (ind. m^{-2}).

variations in the Arctic mesozooplankton community composition at the shelf north of the Polar Front mainly involved ontogenetic development of the copepods and abundant occurrence of meroplankton during summer. However, in the depressions of the shelf north of the polar front, the zooplankton community was very diverse, which contradicts our original hypothesis that the greatest diversity would be expected in areas influenced by the advection of Atlantic waters. The inflow areas only had high diversity during the summer months, but generally lower diversity than the Arctic shelf area, particularly during the winter-early spring.

Ecosystem change may occur in a non-linear fashion as seen in other studies from ice-covered areas (Weydmann et al., 2013), and in the future, we might expect an increased abundance of Atlantic and cosmopolitan species as well as a spread in their distribution also to the shelf area North of the Polar Front. The Atlantic copepod *C. finmarchicus* was the most abundant calanoid on the shelf slope north of Svalbard demonstrating the influential role of Atlantic fauna in the Arctic Ocean ecosystem, but we have still not observed local reproduction of this species in the Arctic Ocean.

Funding

This work was funded by the Research Council of Norway through the project The Nansen Legacy (RCN # 276730).

Declaration of Competing Interest

The authors declare that they have no known competing financial interests or personal relationships that could have appeared to influence the work reported in this paper.

Data availability

Mesozooplankton biodiversity Nansen Legacy Q3: https://data.npolar.no/dataset/f7fd75bc-34d2-4a09-ae90-d27286fcb038, DOI10.21334/npolar.2022.f7fd75bc

Mesozooplankton biodiversity Nansen Legacy Q4: https://data.npolar.no/dataset/97de88ef-3e5e-47de-93ed-5d8f6883c53a, DOI10.21334/npolar.2022.97de88ef

Mesozooplankton biodiversity Nansen Legacy Q1: https://data.npolar.no/dataset/914b8de1-13be-428a-befb-bce6f6f26624, DOI10.21334/npolar.2022.914b8de1

Mesozooplankton biodiversity Nansen Legacy Q2: https://data.npolar.no/dataset/33385ab0-3e2e-4903-9a50-5be2925e3444, DOI10.21334/npolar.2022.33385ab0

Mesozooplankton biodiversity Nansen Legacy JC2-1: https://data.npolar.no/dataset/bb4e2203-bd73-45a1-a861-89b42d1d0d22, DOI10.21334/npolar.2022.bb4e2203

The CTD data used in this study is available at the Norwegian Marine Data Centre NMDC (https://nmdc.no):

Nansen Legacy Q3: https://doi.org/10.21335/NMDC-1107597377
Nansen Legacy Q4: https://doi.org/10.21335/NMDC-301551919
Nansen Legacy Q1: https://doi.org/10.21335/NMDC-1491279668
Nansen Legacy Q2: https://doi.org/10.21335/NMDC-515075317
Nansen Legacy JC2-1: https://doi.org/10.21335/NMDC-2085836005

Acknowledgments

This work was funded by the Research Council of Norway through the project The Nansen Legacy (RCN # 276730). We would like to thank the captain and crew of R/V *Kronprins Haakon* for their excellent support at sea during the Nansen Legacy research cruises. We thank Elisabeth Halvorsen, Amalia Keck, Nadjejda Espinel and Vanesa Pitusi for sampling zooplankton during Q2 and J2-1 cruises.

Appendix A. Supplementary data

Supplementary data to this article can be found online at https://doi.org/10.1016/j.pocean.2023.103133.

References

Aarflot, J.M., Skjoldal, H.R., Dalpadado, P., Skern-Mauritzen, M., 2018. Contribution of *Calanus* species to the mesozooplankton biomass in the Barents Sea. ICES J. Mar. Sci. 75, 2342–2354. https://doi.org/10.1093/icesjms/fsx221.

Aarflot, J.M., Eriksen, E., Prokopchuk, I., Svensen, C., Søreide, J.E., Wold, A., Skogen, M. D., 2023. New insights into the Barents Sea *Calanus glacialis* population dynamics and distribution. Prog. Oceanogr. 217 https://doi.org/10.1016/j.pocean.2023.103106.

Arashkevich, E., Wassmann, P., Pasternak, A., Riser, C.W., 2002. Seasonal and spatial changes in biomass, structure, and development progress of the zooplankton community in the Barents Sea. J. Mar. Syst. 38 (1–2), 125–145. https://doi.org/10.1016/S0924-7963(02)00173-2.

Ardyna, M., Arrigo, K.R., 2020. Phytoplankton dynamics in a changing Arctic Ocean. Nat. Clim. Chang. 10, 892–903. https://doi.org/10.1038/s41558-020-0905-y.

Ardyna, M., Babin, M., Gosselin, M., Devred, E., Rainville, L., Tremblay, J.-É., 2014. Recent Arctic Ocean sea ice loss triggers novel fall phytoplankton blooms. Geophys. Res. Lett. 41, 6207–6212. https://doi.org/10.1002/2014GL061047.

Arrigo, K.R., van Dijken, G.L., 2015. Continued increases in Arctic Ocean primary production. Prog. Oceanogr. 136, 60–70. https://doi.org/10.1016/j.pocean.2015.05.002 0079-6611.

Asbjørnsen, H., Årthun, M., Skagseth, Ø., Eldevik, T., 2020. Mechanisms underlying recent Arctic Atlantification. Geophys. Res. Lett. 47 https://doi.org/10.1029/2020GL088036.

Balazy, K., Boehnke, R., Trudnowska, E., Søreide, J.E., Blachowiak-Samoly, K., 2021. Phenology of *Oithona similis* demonstrates that ecological flexibility may be a winning trait in the warming Arctic. Sci. Rep. 11, 18599. https://doi.org/10.1038/s41598-021-98068-8.

Barth-Jensen, C., Daase, M., Ormańczyk, M.R., Varpe, Ø., Kwasniewski, S., Svensen, C., 2022. High abundances of small copepods early developmental stages and nauplii strengthen the perception of a non-dormant Arctic winter. Polar Biol. 45, 675–690. https://doi.org/10.1007/s00300-022-03025-4.

Basedow, S.L., Sundfjord, A., von Appen, W.-J., Halvorsen, E., Kwasniewski, S., Reigstad, M., 2018. Seasonal variation in transport of zooplankton into the Arctic Basin through the Atlantic Gateway, Fram Strait. Front. Mar. Sci. 5.

Berge, J., Daase, M., Renaud, P.E., Ambrose Jr., W.G., Darnis, G., Last, K.S., Leu, E., Cohen, J.H., Johnsen, G., Moline, M.A., Cottier, F., Varpe, Ø., Shunatova, N., Ba1azy, P., Morata, N., Massabuau, J.-C., Falk-Petersen, S., Kosobokova, K., Hoppe, C.J.M., Weslawski, J.M., Kuklinski, P., Legezynska, J., Nikishina, D., Cusa, M., Kedra, M., Wlodarska-Kowalczuk, M., Vogedes, D., Camus, L., Tran, D., Michaud, E., Gabrielsen, T.M., Granovitch, A., Gonchar, A., Krapp, R., Callesen, T.A., 2015. Unexpected levels of biological activity during the polar night offer new perspectives on a warming Arctic. Curr. Biol. 25, 2555–2561. 10.1016/j.cub.2015.08.024.

Beszczynska-Möller, A., Fahrbach, E., Schauer, U., Hansen, E., 2012. Variability in Atlantic water temperature and transport at the entrance to the Arctic Ocean, 1997–2010. ICES J. Mar. Sci. 69, 852–863. https://doi.org/10.1093/icesjms/fss056.

Blachowiak-Samolyk, K., Kwasniewski, S., Hop, H., Falk-Petersen, S., 2008a. Magnitude of mesozooplankton variability: a case study from the Marginal Ice Zone of the Barents Sea in spring. J. Plankton Res. 30, 311–323. https://doi.org/10.1093/plankt/fbn002.

Blachowiak-Samolyk, K., Søreide, J.E., Kwasniewski, S., Sundfjord, A., Hop, H., Falk-Petersen, S., Hegseth, E.N., 2008b. Hydrodynamic control of mesozooplankton abundance and biomass in northern Svalbard waters (79–81 oN). Deep Sea Res. II 55, 2210–2224. https://doi.org/10.1016/j.dsr2.2008.05.018.

Blachowiak-Samolyk, K., Wiktor, J.M., Hegseth, E.N., Wold, A., Falk-Petersen, S., Kubiszyn, A.M., 2015. Winter tales: the dark side of planktonic life. Polar. Biol. 38, 23–36. https://doi.org/10.1007/s00300-014-1597-4.

Castro de la Guardia, L., Hernández Fariñas, T., Marchese, M., Amargant-Arumí, M., Myers, P.G., Bélanger, S., Assmy, P., Gradinger, R., Duarte, P., accepted. Contrasting seasonal estimates of NPP in the northwest Barents Sea using in situ, satellite and modelling approaches. Prog. Oceanogr. (this volume).

Cavalieri, D.J., Parkinson, C.L., Gloersen, P., Zwally, H., 1996 (updated yearly). Sea Ice concentrations from Nimbus-7 SMMR and DMSP SSM/I-SSMIS Passive Microwave Data. NASA National Snow and Ice Data Center Distributed Active Archive Center, Boulder, Colorado. 10.5067/8GQ8LZQVL0VL.

Clarke, K., R. Gorley (2015). "PRIMER version 7: User manual/tutorial." PRIMER-E 192.

Crews, L., Sundfjord, A., Hattermann, T., 2019. How the Yermak Pass Branch regulates Atlantic Water inflow to the Arctic Ocean. J. Geophys. Res. Oceans 124, 267–280. https://doi.org/10.1029/2018JC014476.

Daase, M., Eiane, K., 2007. Mesozooplankton distribution in northern Svalbard waters in relation to hydrography. Polar Biol. 30, 969–981. https://doi.org/10.1007/s00300-007-0255-5.

Daase, M., Falk-Petersen, S., Varpe, Ø., Darnis, G., Søreide, J.E., Wold, A., Leu, E., Berge, J., Philippe, B., Fortier, L., 2013. Timing of reproductive events in the marine copepod *Calanus glacialis*: a pan-Arctic perspective. Can. J. Fish. Aquat. Sci. 70, 871–884. https://doi.org/10.1139/cjfas-2012-0401.

Daase, M., Varpe, Ø., Falk-Petersen, S., 2014. Non-consumptive mortality in copepods: occurrence of *Calanus* spp. carcasses in the Arctic Ocean during winter. J. Plankton Res. 36, 129–144. https://doi.org/10.1093/plankt/fbt079.

Daase, M., Hop, H., Falk-Petersen, S., 2016. Small-scale diel vertical migration of zooplankton in the High Arctic. Polar. Biol. 39, 1213–1223. https://doi.org/10.1007/s00300-015-1840-7.

Daase, M., Søreide, J.E., 2021. Seasonal variability in non-consumptive mortality of Arctic zooplankton. J. Plankton Res. 43, 565–585. https://doi.org/10.1093/plankt/fbab042.

Dalpadado, P., Ingvaldsen, R.B., Stige, L.C., Bogstad, B., Knutsen, T., Ottesen, G., Ellertsen, B., 2012. Climate effects on Barents Sea ecosystem dynamics. ICES J. Mar Sci. 69, 1303–1316. https://doi.org/10.1093/icesjms/fss063.

Dalpadado, P., Arrigo, K.R., Hjøllo, S.S., Rey, F., Ingvaldsen, R.B., Sperfeld, E., van Dijken, G.L., Stige, L.C., Olsen, A., Ottersen, G., 2014. Productivity in the Barents Sea - Response to recent climate variability. PLoS ONE 9, e95273.

Dalpadado, P., Arrigo, K.R., van Dijken, G.L., Skjoldal, H.R., Bagøien, E., Dolgov, A.V., Prokopchuk, I.P., Sperfeld, E., 2020. Climate effects on temporal and spatial dynamics of phytoplankton and zooplankton in the Barents Sea. Prog. Oceanogr. 185, 102320 https://doi.org/10.1016/j.pocean.2020.102320.

Descôteaux, R., Ershova, E., Wangensteen, O.S., Præbel, K., Renaud, P.E., Cottier, F., Bluhm, B.A., 2021. Meroplankton diversity, seasonality and life-history traits across the Barents Sea Polar Front revealed by high-throughput DNA barcoding. Front. Mar. Sci. 8, 677732 https://doi.org/10.3389/fmars.2021.677732.

Duarte, P., Meyer, A., Moreau, S., 2021. Nutrients in water masses in the Atlantic sector of the Arctic Ocean: Temporal trends, mixing and links with primary production. J. Geophys. Res. Oceans 126. https://doi.org/10.1029/2021JC017413.

Edvardsen, A., Tande, K.S., Slagstad, D., 2003. The importance of advection and production of *Calanus finmarchicus* 2068 in the Atlantic part of the Barents Sea. Sarsia 88, 261–273. https://doi.org/10.1080/00364820310002254.

Ershova, E.A., Kosobokova, K.N., Banas, N.S., Ellingsen, I., Niehoff, B., Hildebrandt, N., Hirche, H.-J., 2021. Sea ice decline drives biogeographical shifts of key *Calanus* species in the central Arctic Ocean. Glob. Chang. Biol. 27, 2128–2143. https://doi.org/10.1111/gcb.15562.

Falk-Petersen, S., Pavlov, V., Timofeev, S., Sargent, J.R., 2007. Climate variability and possible effects on arctic food chains: the role of *Calanus*. In: Ørbæk, J.B., Kallenborn, R., Tombre, I., Hegseth, E.N., Falk-Petersen, S., Hoel, A.H. (Eds.), Arctic-Alpine ecosystems and people in a changing environment. Springer Verlag, Berlin, pp. 147–166.

Gerland, S., Ingvaldsen, R.B., Reigstad, M. Sundfjord, A., Bogstad, B., Chierici, M., Hop, H., Smedsrud, L.H., Stige, L.C., Årthun, M., Berge, J., Bluhm, B.A., Borgå, K., Bratbak, G., Divine, D.V., Eldevik, T., Eriksen, E., Fer, I., Fransson, A., Gradinger, R., Granskog, M.A., Haug, T., Husum, K., Johnsen, G., Jonassen, M.O., Jørgensen, L.L., Kristiansen, S., Larsen, A., Lien, V.S., Lind, S., Lindstrøm, U., Mauritzen, C., Melsom, A., Mernild, S.H., Müller, M., Nilsen, F., Primicerio, R., Renaud, P.E., Søreide, J.E., van der Meeren, G.I., Wassmann, P., 2023. Still Arctic? – The changing Barents Sea. *Elementa: Science of the Anthropocene*. ELEMENTA-D-22-00088R2 (in press).

Gluchowska, M., Dalpadado, P., Beszczynska-Möller, A., Olszewska, A., Ingvaldsen, R.B., Kwasniewski, S., 2017. Interannual zooplankton variability in the main pathways of the Atlantic water flow into the Arctic Ocean (Fram Strait and Barents Sea branches). ICES J. Mar. Sci. 74, 1921–1936. https://doi.org/10.1093/icesjms/fsx033.

Holm-Hansen, O., Riemann, B., 1978. Chlorophyll *a* determination: Improvements in methodology. Oikos 30, 438–447. https://doi.org/10.2307/3543338.

Hop, H., Assmy, P., Wold, A., Sundfjord, A., Daase, M., Duarte, P., Kwasniewski, S., Gluchowska, M., Wiktor, J.M., Tatarek, A., Wiktor Jr., J., Kristiansen, S., Fransson, A., Chierici, M., Vihtakari, M., 2019. Pelagic ecosystem characteristics across the Atlantic Water Boundary Current from Rijpfjorden, Svalbard, to the Arctic Ocean during summer (2010–2014). Front. Mar. Sci. 6, 181. https://doi.org/10.3389/fmars.2019.00181.

Hop, H., Vihtakari, M., Bluhm, B.A., Daase, M., Gradinger, R., Melnikov, I.A., 2021a. Ice-associated amphipods in a pan-Arctic scenario of declining sea ice. Front. Mar. Sci. 8, 743152 https://doi.org/10.3389/fmars.2021.743152.

Hop, H., Wold, A., Meyer, A., Bailey, A., Hatlebakk, M., Kwasniewski, S., Leopold, P., Kuklinski, P., Søreide, J.E., 2021b. Winter-spring development of the zooplankton community below sea ice in the Arctic Ocean. Front. Mar. Sci. 8, 609480 https://doi.org/10.3389/fmars.2021.609480.

Ingvaldsen, R.B., Loeng, H., Asplin, L., 2002. Variability in the Atlantic inflow to the Barents Sea based on a one-year time series from moored current meters. Cont. Shelf Res. 22, 505–519.

Ingvaldsen, R.B., Assmann, K.M., Primicierio, R., Fossheim, M., Polyakov, I.V., Dolgov, A.V., 2021. Physical manifestations and ecological implications of Arctic Atlantification. Nature Rev. Earth Environ. 2, 874–889. https://doi.org/10.1038/s43017-021-00228-x.

Ivanov, V.V., Polyakov. I.V., Dmitrenko, I.A., Hansen, E., Repin, I.A., Kirillov, S.A., Mauritzen, C., Simmons, H., Timokhov, L.A., 2009. Seasonal variability in Atlantic Water off Spitsbergen. Deep Sea Res. I 56, 1-14. 0.1016/j.dsr.2008.07.013.

Ji, R., Ashjian, C.J., Campbell, R.G., Chen, C., Gao, G., Davis, C.S., Cowles, G.W., Beardsley, R.C., 2012. Life history and biogeography of *Calanus* copepods in the Arctic Ocean: An individual-based modeling study. Prog. Oceanogr. 96, 40–56. https://doi.org/10.1016/j.pocean.2011.10.001.

Kosobokova, K.N., Hopcroft, R.R., Hirche, H.-J., 2011. Patterns of zooplankton diversity through the depths of the Arctic's central basins. Mar. Biodiv. 41, 29–50. https://doi.org/10.1007/s12526-010-0057-9.

Kunisch, E.H., Bluhm, B.A., Daase, M., Gradinger, R., Hop, H., Melnikov, I.A., Varpe, Ø., Berge, J., 2020. Pelagic occurrences of the ice amphipod *Apherusa glacialis* throughout the Arctic. J. Plankton Res. 42, 73–86. https://doi.org/10.1093/plankt/fbz072.

Kvile, K.Æ., Ashjian, C., Rubao, J., 2019. Pan-arctic depth distribution of diapausing *Calanus* copepods. Biol. Bull. 237, 76–89. https://doi.org/10.1086/704694.

Kwasniewski, S., Hop, H., Falk-Petersen, S., Pedersen, G., 2003. Distribution of *Calanus* species in Kongsfjorden, a glacial fjord in Svalbard. J. Plankton Res. 25, 1–20.
Laakmann, S., Kochzius, M., Auel, H., 2009. Ecological niches of Arctic deep-sea copepods: Vertical partitioning, dietary preferences and different trophic levels minimize inter-specific competition. Deep Sea Res. I 56, 741–756. https://doi.org/10.1016/j.dsr.2008.12.017.
Leu, E., Wiktor, J., Søreide, J.E., Berge, J., Falk-Petersen, S., 2010. Increased irradiance reduces food quality of sea ice algae. Mar. Ecol. Prog. Ser. 411, 49–60. https://doi.org/10.3354/meps08647.
Leu, E., Søreide, J.E., Hessen, D.O., Falk-Petersen, S., Berge, J., 2011. Consequences of changing sea-ice cover for primary and secondary producers in the European Arctic shelf seas: Timing, quantity, and quality. Prog. Oceanogr. 90, 18–32. https://doi.org/10.1016/j.pocean.2011.02.004.
Leu, E., Mundy, C.J., Assmy, P., Campbell, K., Gabrielsen, T.M., Gosselin, M., Juul-Pedersen, T., Gradinger, R., 2015. Arctic spring awakening – Steering principles behind the phenology of vernal ice algal blooms. Prog. Oceanogr. 139, 151–170. https://doi.org/10.1016/j.pocean.2015.07.012.
Lind, S., Ingvaldsen, R.B., 2012. Variability and impacts of Atlantic Water entering the Barents Sea from the north. Deep Sea Res. I 62, 70–88. https://doi.org/10.1016/j.dsr.2011.12.007.
Lind, S., Ingvaldsen, R.B., Furevik, T., 2018. Arctic warming hotspot in the northern Barents Sea linked to declining sea-ice import. Nat. Clim. Chang. 8, 634–639. https://doi.org/10.1038/s41558-018-0205-y.
Lischka, S., Hagen, W., 2005. Life history and seasonal variability in abundances of *Pseudocalanus minutus* (Calanoida) and *Oithona similis* (Cyclopoida) in the Arctic Kongsfjord (Svalbard). Polar Biol. 28, 910–921. https://doi.org/10.1007/s00300-005-0017-1.
Lischka, S., Hagen, W., 2007. Seasonal lipid dynamics of the copepods *Pseudocalanus minutus* (Calanoida) and *Oithona similis* (Cyclopoida) in the Arctic Kongsfjorden (Svalbard). Mar. Biol. 150, 443–454. https://doi.org/10.1007/s00227-006-359-4.
Lundesgaard, Ø., Sundfjord, A., Lind, S., Nilsen, F., Renner, A.H.H., 2022. Import of Atlantic Water and sea ice controls the ocean environment in the northern Barents Sea. Ocean Sci. 18, 1389–1418. https://doi.org/10.5194/os-18-1389-2022.
MacKenzie, K.M., Lydersen, C., Haug, T., Routti, H., Aars, J., Andvik, C.M., Borgå, K., Fisk, A.T., Biuw, M., Lowther, A.D., Lindström, U., Kovacs, K.M., 2022. Ecological niches of marine mammals in the European Arctic. Ecol. Ind. 136, 108661 https://doi.org/10.1016/j.ecolind.2022.108661.
Mańko, M.K., Gluchowska, M., Weydmann-Zwolicka, A., 2020. Footprints of Atlantification in the vertical distribution and diversity of gelatinous zooplankton in the Fram Strait (Arctic Ocean). Prog. Oceanogr. 189, 102414 https://doi.org/10.1016/j.pocean.2020.102414.
Melle, W., Skjoldal, H.R., 1998. Reproduction and development of *Calanus finmarchicus, C. glacialis* and *C. hyperboreus* in the Barents Sea. Mar. Ecol. Prog. Ser. 169, 211–228.
Oziel, L., Sirven, J., Gascard, J.-C., 2016. The Barents Sea frontal zones and water masses variability (1980–2011). Ocean Sci. 12, 169–184. https://doi.org/10.5194/os-12-169-2016.
Pedersen, T., 2022. Comparison between trophic positions in the Barents Sea estimated from stable isotope data and a mass balance model. Front. Mar. Sci. 9, 813977 https://doi.org/10.3389/fmars.2022.813977.
Polyakov, I.V., Ingvaldsen, R.B., Pnysushkov, A.V., Bhatt, U.S., Francis, J.A., Janout, M., Kwok, R., Skagseth, Ø., 2023. Fluctuating Atlantic inflows modulate Arctic atlantification. Science 381, 972–979. https://doi.org/10.1126/science.adh515.
Postel, L., 2000. Biomass and abundance. In: Harris, R., Wiebe, P., Lenz, J., Skjoldal, H. R., Huntley, M. (Eds.), ICES Zooplankton Methodology Manual. Academic Press, London, p. 684.
Rantanen, M., Karpechko, A.Y., Lipponen, A., Nordling, K., Hyvärinen, O., Ruosteenoja, K., Vihma, T., Laaksonen, A., 2022. The Arctic has warmed nearly four times faster than the globe since 1979. Commun. Earth Environ. 3, 168. https://doi.org/10.1038/s43247-022-00498-3.
Renaut, S., Devred, E., Babin, M., 2018. Northward expansion and intensification of phytoplankton growth during the early ice-free season in Arctic. Geophys. Res. Lett. 45 https://doi.org/10.1029/2018GL078995.
Renner, A.H.H., Sundfjord, A., Janout, M.A., Ingvaldsen, R.B., Beszczynska Möller, A., Pickart, R.S., Pérez-Hernández, M.D., 2018. Variability and redistribution of heat in the Atlantic water boundary current north of Svalbard. J. Geophys. Res. Oceans 123, 6373–6391. https://doi.org/10.1029/2018JC013814.
Rombouts, I., Beaugrans, G., Ibanez, F., Gasparini, S., Chiba, S., Legendre, L., 2009. Global latitudinal variations in marine copepod diversity and environmental factors. Proc. R. Soc. 276, 3053–3062. https://doi/101098/rspb.2009.0742.
Siwertsson, A., Husson, B., Arneberg, P., Assmann, K., Assmy, P., Aune, M., Bogstad, B., Børsheim, K.Y., Cochrane, S., Daase, M., Fauchald, P., Frainer, A., Fransson, A., Hop, H., Höffle, H., Gerland, S., Ingvaldsen, R., Jentoft, S., Kovacs, K.M., Leonard, D.M., Lind, S., Lydersen, C., Pavlova, O., Peuchet, L., Primicerio, R., Renaud, P.E., Solvang, H.K., Skaret, G., van der Meeren, G., Wassmann, P., Øien, N., 2023. Panel-based assessment of ecosystem condition of Norwegian Barents Sea Shelf Ecosystems. Rapport fra Havforskningen 2023-14. ISSN:1893-4536.
Šmilauer, P., and Lepš, J., 2014. Multivariate Analysis of Ecological Data using CANOCO 5 (2nd ed.). Cambridge: Cambridge University Press. 10.1017/CBO9781139627061.
Søreide, J.E., Hop, H., Falk-Petersen, S., Gulliksen, B., Hansen, E., 2003. Macrozooplankton communities and environmental variables in the Barents Sea marginal ice zone in late winter and spring. Mar. Ecol. Prog. Ser. 263, 43–64.
Søreide, J.E., Leu, E., Berge, J., Graeve, M., Falk-Petersen, S., 2010. Timing of blooms, algal food quality and *Calanus glacialis* reproduction and growth in a changing Arctic. Glob. Chang. Biol. 16, 3154–3163. https://doi.org/10.1111/j.1365-2486.2010.02175.x.
Stroeve, J., Notz, D., 2018. Changing state of Arctic sea ice across all seasons. Environ. Res. Lett. 13, 103001 https://doi.org/10.1088/1748-9326/aade56.
Sundfjord, A., Assmann, K.M., Lundesgaard, Ø., Renner, A.H.H., Lind, S., Ingvaldsen, R. B., 2020. Suggested water mass definitions for the central and northern Barents Sea, and the adjacent Nansen Basin. The Nansen Legacy Report Series. https://doi.org/10.7557/nlrs.5707.
Tarling, G.A., Freer, J.J., Banas, N.S., Belcher, A., Blackwell, M., Castellani, C., Cook, K. B., Cottier, F.R., Daase, M., Johnson, M.L., Last, K.S., Lindeque, P.K., Mayor, D.J., Mitchell, E., Parry, H.E., Speirs, D.C., Stowasser, G., Wootton, M., 2022. Can a key boreal *Calanus* copepod species now complete its life-cycle in the Arctic? Evidence and implications for Arctic food-webs. Ambio 51, 333–344. https://doi.org/10.1007/s13280-021-01667-y.
Våge, S., Basedow, S.L., Tande, K.S., Zhou, M., 2014. Physical structure of the Barents Sea Polar Front near Storbanken in August 2007. J. Mar. Syst. 130, 256–262. https://doi.org/10.1016/j.jmarsys.2011.11.019.
Van Engeland, T., Bagøien, E., Wold, A., Cannaby, H.A., Majaneva, S., Vader, A., Rønning, J., Handegard, N.O., Dalpadado, P., Ingvaldsen, R.B., 2023. Diversity and seasonal development of large zooplankton along physical gradients in the Arctic Barents Sea. Prog. Oceanogr. 216, 103065 https://doi.org/10.1016/j.pocean.2023.103065.
Wassmann, P., Reigstad, M., Haug, T., Rudels, B., Carroll, M.L., Hop, H., Gabrielsen, G. W., Falk-Petersen, S., Denisenko, S.G., Arashkevich, E., Slagstad, D., Pavlova, O., 2006. Food webs and carbon flux in the Barents Sea. Prog. Oceanogr. 71, 232–287. https://doi.org/10.1016/j.pocean.2006.10.003.
Wassmann, P., Kosobokova, K.N., Slagstad, D., Drinkwater, K.F., Hopcroft, R.R., Moore, S.E., Ellingsen, I., Nelson, R.J., Carmack, E., Popova, E., Berge, J., 2015. The contiguous domains of Arctic Ocean advection: Trails of life and death. Prog. Oceanogr. 139, 42–65. https://doi.org/10.1016/j.pocean.2015.06.011 0079-6611.
Wassmann, P., Slagstad, D., Ellingsen, I., 2019. Advection of mesozooplankton Into the Northern Svalbard Shelf Region. Front. Mar. Sci. 6, 458. https://doi.org/10.3389/fmars.2019.00458.
Weydmann, A., Søreide, J.E., Kwaśniewski, S., Leu, E., Falk-Petersen, S., Berge, J., 2013. Ice-related seasonality in zooplankton community composition in a high Arctic fjord. J. Plankton Res. 35, 831–842. https://doi.org/10.1093/plankt/fbt031.